
**TRIBHUVAN UNIVERSITY**

**INSTITUTE OF ENGINEERING**

**PULCHOWK CAMPUS**

**THESIS NO: 079/MSPDE/011**

# Harmonic Analysis and Its Mitigation for Integrating EV Charging Stations on Distribution System Network

**by**

**Isha Tiwari**

**A THESIS**

**SUBMITTED TO THE DEPARTMENT OF ELECTRICAL ENGINEERING IN PARTIAL FULFILLMENT OF THE REQUIREMENT FOR THE DEGREE OF MASTER OF SCIENCE IN POWER ELECTRONICS AND DRIVES ENGINEERING**

**DEPARTMENT OF ELECTRICAL ENGINEERING**

**PULCHOWK CAMPUS**

**LALITPUR, NEPAL**

**APRIL 2025**

**Harmonic Analysis and Its Mitigation for Integrating EV Charging Stations on Distribution System Network**

By

Isha Tiwari

PUL079MSPDE011

Thesis Supervisor

Jeetendra Chaudhary

Associate Professor, Department of Electrical Engineering Pulchowk Campus, IOE, Tribhuvan University, Nepal

Dr. Laxman Maharjan

Department of Electrical Engineering, Pulchowk Campus, IOE, Tribhuvan University, Nepal

A thesis submitted to the Department of Electrical Engineering in partial fulfilment of the requirements for the Degree of Master in Power Electronics and Drives Engineering

Department of Electrical Engineering

Institute of Engineering, Pulchowk Campus, Tribhuvan University

Lalitpur, Nepal

April 2025

## COPYRIGHT©

## CERTIFICATE OF APPROVAL

The undersigned certify that they have read and recommended to the Institute of Engineering for acceptance, a thesis entitled "**Harmonic Analysis and Its Mitigation for Integrating EV Charging Stations on Distribution System Network**", submitted by **Isha Tiwari** in partial fulfillment of the requirement for the degree of **Master of Science in Power Electronics and Drives Engineering.**

Assoc. Prof. Jeetendra Chaudhary
Department of Electrical Engineering
Pulchowk Campus, Lalitpur
(Supervisor)

Dr. Laxman Maharjan
Former Assistant Manager
Corporate R&D Headquarters, Fuji Electric Co., Ltd., Japan
(Supervisor)

Prof. Dr. Bhupendra Bimal Chhetri
Department of Electrical and Electronics Engineering
Kathmandu University, Dhulikhel
(External Examiner)

Assoc. Prof. Jeetendra Chaudhary
Program Coordinator
M. Sc. Power Electronics and Drives Engineering
Pulchowk Campus, Lalitpur

Assoc. Prof. Dr. Basanta K. Gautam
Head of Department
Department of Electrical Engineering
Pulchowk Campus, Lalitpur

April 2025

**ACKNOWLEDGEMENT**

I would like to express my heartfelt gratitude to all those who have contributed to the successful completion of the thesis on "Harmonic analysis and Its mitigation for Integrating EV Charging Stations on Distribution System Network ". This thesis journey has been thrilling, but with constant collaboration, guidance, encouragement, and support from the numerous individuals who made this moment possible, to completed this journey.

First and foremost, I express my deepest gratitude to my thesis supervisor, Assoc. Prof Jeetendra Chaudhary and Dr. Laxman Maharjan for their invaluable mentorship, constructive feedback, and multidisciplinary support throughout this research tenure. Their expertise in power electronics and passion to share knowledge and foster innovation have been a constant source of inspiration.

I am immensely grateful to the Department of Electrical Engineering, faculty members of Electrical Engineering from the Institute of Engineering, for their guidance and encouragement during my studies, also a special thanks to the technical staff, laboratory assistants, and my colleagues and peers for their help and support during my time. I would like to thank Sajha Yatayat and NEA for allowing me to oversee the charging infrastructure and technology and for providing me with the required data, which has made me more motivated and passionate about my work.

Finally, I owe a debt of gratitude to my friends and family for their unconditional love, patience, and encouragement. This thesis is a testament to the collective effort of everyone mentioned above, and I am truly thankful for their contributions to my academic and personal growth.

## ABSTRACT

In automobile industry Electric Vehicles (EVs) are getting more attention because of its lower emissions in carbon dioxide, lesser operation costs more ease in maintenance. The distribution network feature is more affected by the huge demand of electrical energy as the number of EV rose. Besides with the introduction of EV infrastructure distribution system has faced a lot of difficulties in power quality such as harmonic distortion. With the implementation of advanced power electronics devices in charger's variations in loads occurs, this leads to change in the sinusoidal pattern in terms of electrical parameters such as current and voltage waveforms.

This dissertation investigates the impact of electric vehicle (EV) charging stations on total harmonic distortion (THD) within a real-world distribution feeder. The study centres around the distribution network in the Sanepa area, where a SAPF. To suppress harmonic currents at the point of common coupling, a shunt active power filter based on the instantaneous reactive power theory is utilized. The implemented method demonstrates a substantial improvement, reducing THD from 27.31% to 1.23%. All system modelling and simulations are conducted using the MATLAB/Simulink environment.

## TABLE OF CONTENTS

## LIST OF TABLES

## LIST OF FIGURES

## LIST OF ABBREVIATIONS

| | |
|---|---|
| AC | Alternating Current |
| APF | Active Power Filter |
| DC | Direct Current |
| DFT | Discrete Fourier Transform |
| EV | Electric Vehicle |
| EVCS | Electric Vehicle Charging Station |
| FFT | Fast Fourier Transform |
| ICE | Internal Combustion Engine |
| PCC | Point of Common Coupling |
| SAPF | Shunt Active Power Filter |
| SMPS | Switching Mode Power Supply |
| THD | Total Harmonic Distortion |
| VSI | Voltage Source Inverter |

# CHAPTER 1: INTRODUCTION

## 1.1. Background

With the increasing concept of clean and green energy, vehicles using fuel are slowly decreasing, and electric vehicle (EVs) are increasing rapidly. Since they don't emit any direct pollutants, EVs has a considerably lesser detrimental effect on the environment and public health than internal combustion engine vehicles (ICEVs). The decline in air quality is primarily driven by emissions from vehicle exhausts, particularly nitrogen oxides (NOx) and particulate matter (PM). Battery electric vehicles (BEVs) cut PM emissions by a factor of four and NOx emissions by a factor of twenty when seen from a well-to-wheel perspective. Because of this, EVs are essential for slowing down climate change, improving public health, and inspiring the growth of intelligent, sustainable urban regions [1].

In recent years, EVs including electric bikes and cars, have gained significant popularity as a preferred mode of transportation across both urban and rural regions. Compared to internal combustion (IC) engine vehicles, EVs are considered more environmentally sustainable and eco-friendly. Due to the popularity of EVs, their use grows by more than 50% by the year 2024. According to the International Energy Agency (IEA), the global stock of EVs has seen substantial growth over the past decade, reaching 10 million in 2022 and projected to rise to 30 million by 2030. Recent progress in EV charging technology has been remarkable. The industry is increasingly embracing innovations like 350kW DC fast chargers and wireless charging systems, both of which are emerging as key developments in the field [1].

Electric vehicles rely on rechargeable batteries to power their systems, and electric vehicle charging stations (EVCS) draw electricity from the utility grid to charge these batteries. To enable rapid charging, these stations incorporate high-speed power converters, sophisticated filtering networks, and advanced control schemes—all of which exhibit pronounced nonlinear behaviour. As the EV market accelerates, the expansion of reliable charging infrastructure has become a backbone for broader adoption. Yet, the existing rollout of charging networks worldwide remains uneven and often falls short of demand in both reach and performance. This study also reviews the global status of charging infrastructure development, identifies the current challenges and opportunities, and proposes relevant recommendations for improvement. This

study is expected to offer meaningful insights and direction for policymakers, industry professionals, and researchers, supporting the continued growth and advancement of the electric vehicle (EV) sector.

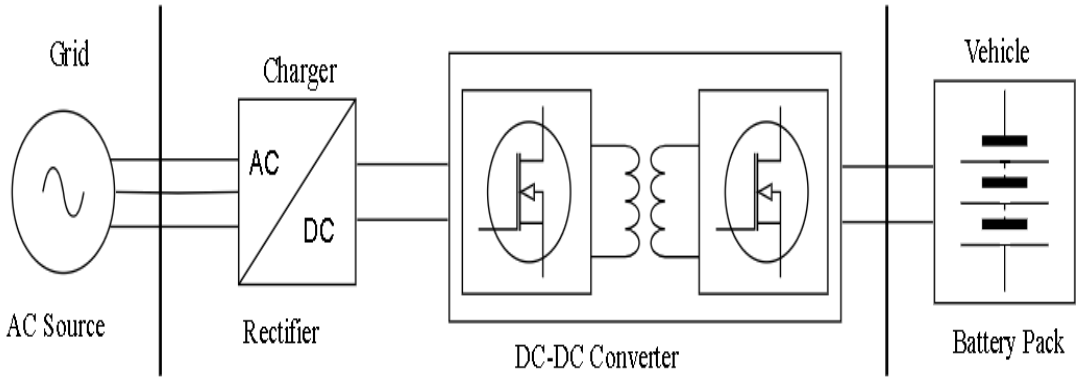


**Figure 1.1**: Electric Vehicle Connection to Grid

### 1.1.1 Evolution of EV charging infrastructure

The development of EV charging stations has progressed in multiple phases:

- Early Stage (2000s-2010s): Initial charging infrastructure focused on slow AC charging for home and commercial applications.
- Expansion (2010s-2020s): Adoption of fast DC chargers (such as CCS, CHAdeMO, GBT, and Tesla Superchargers), expected to offer meaningful insights and direction for policymakers, industry professionals, and researchers, supporting the continued growth and advancement of the electric vehicle (EV) sector.
- Smart Charging & Vehicle to Grid (2020s and beyond): Integration of renewable energy, battery storage, and V2G capabilities to enhance grid stability and efficiency.

### 1.1.2 Components of an EV charging station

These components handle the power supply and regulate electricity flow from the grid to the EV.

**I. Power Source**

Most charging stations are connected to the main electricity grid. It might be single phase or three phase depending upon residential or commercial/fast chargers respectively. Renewable energy is increasingly being integrated as a primary or

supplementary power source for electric vehicle (EV) charging stations, offering a sustainable solution to reduce carbon emissions associated with transportation. Solar photovoltaic (PV) systems are the most commonly used, often installed on station canopies or nearby land to convert sunlight into electricity, which is then used directly or stored in battery energy storage systems (BESS) for later use. According to research published in Renewable and Sustainable Energy Reviews, solar-powered charging reduces reliance on the grid, enhances energy resilience, and reduces long-term operational costs. Though less common, wind energy is also being explored, especially in rural or high-wind areas. Hybrid systems combining solar, wind, and BESS further improve reliability. Additionally, smart grid integration and energy management systems allow for demand response and optimized energy flow between renewable sources, the grid, and EVs. This shift toward renewables in EV infrastructure supports global goals for decarbonization and energy independence. Batteries can be integrated to support peak demand and enable vehicle-to-grid operations.

**II. Transformer**

It steps down high-voltage grid power (typically 11kV or 33kV) to lower voltages suitable for charging (400V or 230V). This 400 V output, typically three-phase, is ideal for commercial and public EV charging stations, especially those using fast or high-power chargers. The transformer not only reduces voltage but also isolates the charging system from the high-voltage grid, enhancing safety and reliability.

**III. Power Electronics (AC/DC Converters & Inverters)**

An AC/DC rectifier converts alternating current (AC) from the grid into direct current (DC), while a Buck/Boost converter adjusts the DC voltage level either increasing or decreasing it to match the requirements of the battery. In fast charging (DC fast chargers), high-power rectifiers (rated from 50 kW to 350 kW) are used to directly supply DC to the EV. Some chargers may include power factor correction circuits to improve efficiency and reduce harmonic distortion.

- AC Chargers (On-board or Off-board): Directly supply AC power, and the EV's onboard charger (OBC) converts it to DC.
- DC Fast Chargers (Off-board): Convert AC to DC externally and directly charge the EV battery, allowing much faster charging.

- Bidirectional Converters (for V2G and V2H applications): Allow power flow from EV to grid (V2G).

### 1.1.3 EV charging station in Nepal

Nepal has been making significant strides in promoting electric vehicles (EVs) as part of its commitment to sustainable energy and reducing carbon emissions. The Nepal Electricity Authority (NEA) has been at the forefront of this initiative, supporting the development of EV charging infrastructure across the country. Nepal currently has 62 operational EV charging stations under the Nepal Electricity Authority (NEA). Among these, 30 stations utilize the CCS-2 charging standard, while 32 follow the GB/T standard. Each station has a capacity of 142 kW, ensuring fast and efficient charging for electric vehicles. This distribution accommodates a wide range of EVs, supporting both major charging standards. NEA has approved applications for an additional 750 charging stations across various locations in Nepal, with a total proposed capacity of 105.32 MW. Of this, 60 MW has already been installed. These charging stations have taken transformer support from NEA, and they are also under the NEA Charging Station Customer group. The total capacity of NEA-operated charging stations stands at 8.8 MW. Additionally, 10.5 MW of charging stations have been installed by private companies, such as TATA Motors, which are not connected to NEA's Charging Station customer group but are in other customer groups, like the commercial user group. In total, Nepal has an installed charging capacity of 78.8 MW, collectively supplying an average of 322,300 units of electricity per day (source-NEA).

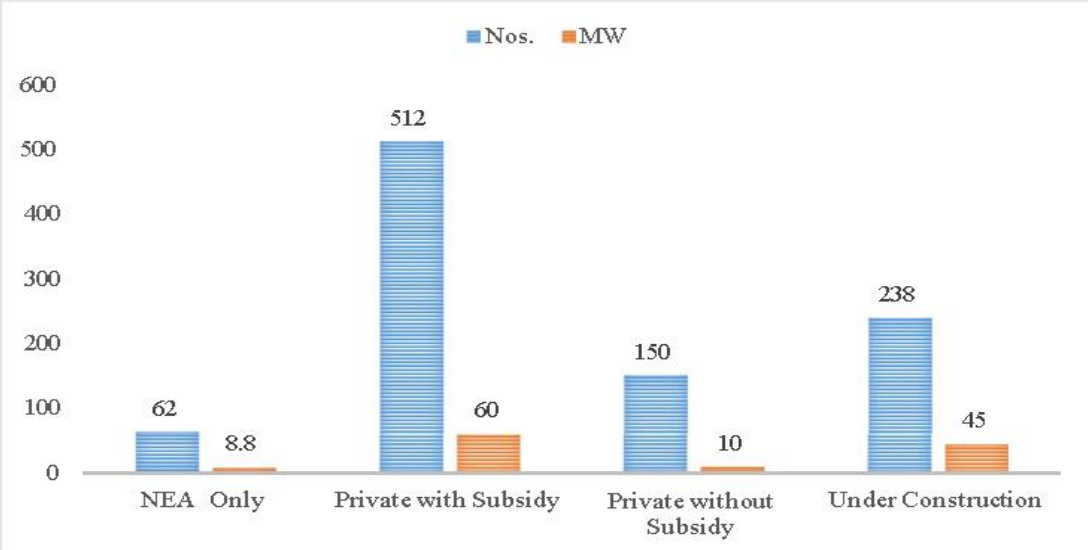


**Figure 1.2**: Status of EV Charging Stations in Nepal

## 1.2. Problem Statement

The growing integration of electric vehicle (EV) charging stations into the distribution network has resulted in notable power quality challenges, mainly caused by harmonic distortions. EV chargers, mainly DC chargers, utilize power electronic converters that introduce non-linear currents, resulting in harmonics that distort the voltage and current waveforms. These harmonics can negatively impact grid performance by increasing THD, causing excessive losses and reducing the lifespan of electrical components such as transformers. These effects are further exacerbated in Nepal's distribution system due to its limited infrastructure capacity, lack of widespread harmonic standards enforcement. Conventional passive harmonic filters have limitations in flexibility, tuning accuracy, and dynamic adaptability to varying load conditions. Passive filters require large components (inductors and capacitors), making them bulky and difficult to integrate into modern systems. To address this challenge, the Shunt Active Power Filter has emerged as an effective solution for harmonic mitigation in EV charging stations. APFs dynamically detect and inject compensating currents to cancel out harmonics in real-time.

## 1.3. Objectives

The primary aim of this study is to evaluate and analyse the harmonic distortion introduced by electric vehicles charging stations on the practical distribution feeder and develop an effective mitigation strategy.

The specific objectives of the study are as follows:

- to develop the model of the real-world distribution feeder (Sanepa feeder) in MATLAB/Simulink and to integrate the charging station of Sajha Yatayat
- To design and implement An SAPF is employed to mitigate power system harmonics

## 1.4. Scope of Thesis

This research focuses on assessing the harmonic distortion caused by the EV charging station on the Sanepa Feeder. The study will involve the modelling of the feeder with integrated EV chargers using MATLAB/Simulink to perform harmonic analysis. A shunt active power filter (SAPF) will be developed and simulated to reduce harmonic distortion and enhance the overall power quality of the system. The research findings

will provide insights into improving power quality in Nepal's distribution system, enabling reliable EV charging infrastructure deployment.

### 1.5. Outline of the thesis

This dissertation is organized into five chapters. This section gives a brief outline of each chapter and the contents of each has.

**Chapter 1:** It gives the background of the dissertation. The problem statement is mentioned along with the main and specific objectives. The scope of thesis explains about the works that has been done in methodology section. This section also covers the limitations of the thesis.

**Chapter 2:** It explores the required literature review done for the dissertation, including fundamentals of harmonics, impacts of harmonics on electrical equipment, different types of filters, and power quality issues. It describes the control mechanism and operation of the shunt active power filter

**Chapter 3:** It describes the research methodology of the dissertation, including the modelling approach used and the workflow of the thesis. The processes that is followed to compute the harmonics and its impact analysis are mentioned.

**Chapter 4:** It discusses the obtained results from the simulation and shows the reliability of the chosen method.

**Chapter 5:** It concludes the research work along with mentioning the objectives.

Finally, this thesis will end with a list of references that were used while carrying out the research.

### 1.6. Limitations of the thesis

The research will be conducted through simulations. And it focuses only on the Sanepa feeder and does not account for other feeders in the distribution network that may also be affected by EV charging. This research specifically concentrates on harmonic distortion and does not address other power quality issues such as voltage sags, swells, or flickers. The exact modelling of the charger used is not done which may lead to reduced accuracy in the simulation results. Without the detailed incorporation of the precise electrical characteristics and dynamic behaviour of the actual charger, the system's response, particularly in terms of power quality and harmonic distortion, may not fully reflect real-world performance. This simplification could result in deviations between simulated outcomes and practical observations. The SAPF control strategies

considered in this study are Instantaneous PQ theory, which may not fully account for future advancements in filtering techniques or artificial intelligence-based control methods.

# CHAPTER 2: LITERATURE REVIEW

## 2.1. Overview

Distribution feeders are critical components of electrical distribution systems that transport power from substations to end users. They consist of overhead and underground conductors, transformers, circuit breakers, and protection devices. The design and operation of distribution feeders aim to ensure reliable and efficient power delivery while minimizing losses and maintaining power quality.

Contemporary distribution networks are advancing with the incorporation of renewable energy sources (RES), including photovoltaic (PV) and wind energy systems. The IRENA's worldwide plan stated that renewable energy consumption will increase from 20% to 40% till 2050 and the output from renewable energy sources will increase by two-third. Besides 2050 the solar generation and wind energy production will donate three times as much as from 20% to 60%. Different actions have been brought in front for effective implementation and to prevent rapid extension of ICEVs [2]. Moreover, as the electricity demand from EVs can be rapidly introduced or withdrawn from the power grid, electrical infrastructure such as power generation units and transformer systems become particularly susceptible to fluctuations in system frequency. Hence, in response to the rapid rise in EV adoption, the power grid requires substantial development to keep pace. To manage the high costs associated with overhauling or enhancing the current electrical infrastructure, robust government support through incentives is crucial. Deploying generation units strategically near the expanding EV charging infrastructure, along with optimized EV scheduling, offers a viable approach to meeting increased energy demands. Additionally, the battery pack and power electronics converter are key components when tapping into power from EVs' onboard chargers.

Due to the presence of distributed energy sources, diverse load types, and energy conversion devices, a microgrid or distributed power plant is inherently more complex and nonlinear compared to a conventional power plant. Chemical energy, thermodynamics, and electrodynamics are all intertwined. Power quality issues are more complicated since consumer-side power quality has a direct impact on production

safety and power efficiency. The widespread adoption of electric vehicles (EVs) is likely to significantly alter residential power consumption patterns, as charging a single EV can be roughly equivalent to adding the power demand of two additional households to the distribution network [3].

### 2.2. Harmonics in Power Systems

Harmonics are non-sinusoidal components in electrical waveforms that arise due to nonlinear loads such as power electronic devices, transformers, and fluorescent lighting. These harmonics distort voltage and current waveforms, leading to reduced power quality, increased losses, overheating of equipment, and malfunction of sensitive electronic devices.

Common sources of harmonics in distribution feeders include:

- Power electronic converters (e.g., inverters, rectifiers)
- Adjustable speed drives (ASDs)
- Uninterruptible power supplies (UPS)
- Nonlinear industrial loads

### 2.3. Effects of Harmonic Distortions in Power Systems:

Harmonics are generally undesirable in electrical power systems, as they adversely affect both the equipment and the overall operation of the system. Resonance in a power system network can be generated via harmonics[4].

#### I. Resonance

Capacitors used for power factor correction can resonate with harmonic frequencies in the system, potentially resulting in excessive currents that may damage the capacitors. Resonance occurs when the the circuit's capacitive and inductive reactance become equal in magnitude, allowing a specific frequency to dominate the system. In series resonance, the impedance is low, while in parallel resonance, the impedance is high at the resonant frequency. Power factor correction capacitor performance is hindered by harmonic resonance.

- Parallel resonance raises harmonic voltages and harmonic currents while providing high impedance at the resonance frequency.
- The series resonance causes higher value of capacitor current when the harmonic voltages is lesser.

- The interaction between the fundamental frequency and direct current components within the converter control system gives rise to a composite resonant frequency that is non-integer in nature.

**II. Poor Damping**

When harmonics are present, a slight negative impedance or resistance may be added by SMPS or variable speed drive motors. As voltage increases, it lowers current, which lowers the system's damping or broadband energy absorption capacity. Unwanted variations in damping level affect the degree to which certain electrical equipment operate, particularly various measuring and regulating devices.

**III. Effects on Rotating Machine**

Harmonic loss: Harmonic voltage and current contribute to increased losses in various parts of an A.C. machine, including the stator windings, rotor circuit, and the laminated cores of both stator and rotor. Typically, these losses exceed the pure D.C. resistance losses due to additional effects such as eddy currents and the skin effect inherent in AC operation. The existence of harmonics amplifies both copper losses (in conductors) and core losses (in magnetic materials), leading to excessive heat generation. Consequently, this not only causes thermal stress but also lowers the overall efficiency of the machine.

Harmonic torque: An AC machine's stator's harmonic currents create additional magnetic fields that may cause electromagnetic induction to cause a motoring action (positive harmonics slip Sn). This leads to shaft torques that align with the velocities of the harmonic fields. Consequently, the positive sequence components of the harmonics generate shaft torques that aid in shaft rotation, while the negative sequence components produce torques that oppose the rotation

Speed torque characteristics: Every harmonic plays a role in generating magnetic forces within the machine. The existence of these harmonics influences the machine’s speed and torque behaviour, leading to alterations in its overall performance characteristics.

Cogging: Cogging refers to the inability of an IM to accelerate to its regular operating speed, which happens when an unchanging operating point is established at a lower frequency, preventing the motor from gaining sufficient momentum.

Voltage stress: Harmonic voltages contribute to greater stress on insulating materials.

## IV. Impact on transformers

RMS Current: Due to the increase in current harmonics distortion in the transformer it results in a higher RMS peak value, which leads to the increased heating within the transformer.

Core loss: Both the eddy current loss and hysteresis current losses in the laminations are increased due to harmonic voltage. The supply voltage's harmonics, the magnetic circuit, and the core material’s design specifications all affect how substantially core loss occurs.

Copper loss: Harmonic currents lead to an increase in copper losses. The loss is primarily determined by load's harmonics and the winding's effective AC resistance. Copper loss increases temperature which creates hot spots in that transformer.

Stress: The stresses of the insulation increase due to the voltage harmonics.

Core vibration: Small core vibrations are exacerbated by harmonics of current and voltage.

Saturation problem: Additional harmonic voltage might occasionally end up in core saturation.

## V. Effects on the Transmission System

Skin effect and Proximity effect: This type of effects is frequency-dependent, and the presence of harmonics amplifies them. Consequently, the effective AC resistance rises when harmonics are present.

Loss: The presence of additional harmonic currents leads to increased copper losses in the transmission system and diminishes its overall power transmission capacity. The formula to calculate copper loss is expressed by $\sum_{n=2}^{\alpha} In^2\, Rn$, where $I_n$ represents the nth harmonic current, and $R_n$ is the system resistance at that specific harmonic frequency.

Voltage drops: Harmonic currents generate voltage drops across various circuit impedances. Consequently, systems with high impedance referred to as weak systems experience lower fault levels and more severe voltage disturbances. In contrast, stiff

systems with low impedance exhibit higher fault levels and minimal voltage disturbances.

Dielectric stress: Harmonic voltages elevate the dielectric stress experienced by transmission line cables. This stress is directly proportional to the peak value of the applied voltage. An increase in dielectric stress results in a corresponding decrease in the dielectric strength of the insulation material. This degradation not only shortens the operational lifespan of the cables but also increases the likelihood of faults, thereby escalating maintenance requirements and associated repair costs.

Corona: The initiation and extinction levels of corona discharge are affected by the peak-to-peak voltage of the system, which is determined by the phase relationship between the harmonic components and the fundamental frequency. The presence of harmonic voltages contributes to an increase in the overall peak voltage, thereby affecting the corona characteristics of the transmission system.

**VI. Effects on Capacitor Banks**

Issues related to distortion usually manifest initially on the power bank of the capacitor. Under conditions of peak voltage harmonics, the capacitor bank may enter a state of resonance, during which the flow of current through the bank becomes significantly large, resonance condition is especially significant when dominant monotonic harmonics are present, with the eleventh harmonic being notably affected which becomes superimposed on the fundamental frequency, thereby impacting the overall behaviour of the capacitor bank. As a result, the root mean square (RMS) current during resonance often exceeds the capacitor's rated RMS current, potentially compromising its performance and operational lifespan. The IEEE Standard for Shunt Power Capacitors (IEEE Standard 18-2002) [5] .It outlines the following continuous capacitor ratings:

- 135% of the total KVAR.
- 110% of the rated RMS voltage value, along with the harmonics once the transient effects have dissipated.
- The capacitor is subjected to a voltage level reaching 120% of the nominal value, inclusive of harmonic content.

Among the harmonic components, the fifth and seventh harmonics are most prominent in affecting the capacitor. The distorted voltage waveform consists of 4% fifth harmonic and 3% seventh harmonic components. As a result, this leads to a 20% fifth harmonic current and a 21% seventh harmonic current flowing through the capacitor. Despite these distortions, all resulting harmonic values remain within acceptable standard limits under the given conditions.

**VII. Effect on Measuring Instruments**

Power usage in the distribution system is usually measured by utilities in two ways: the total amount of power consumed and the maximum amount of energy used in a certain period of time. As an outcome, both demand and energy expenses are included in billing for bigger corporate customers. In contrast, residential users are typically only charged for the power they use. The costs of producing and delivering electricity are referred to as the power price, and they are determined by the time spent in kWh. The second component's calculation, the KVA rate, represents the distributor's rates for keeping enough energy capacity to satisfy every user's power consumption requirement. KVA billing is often determined by the maximum KVA demand recorded over a peak period of fifteen or thirty minutes, expressed in kilowatts (kW). With the application of watthour device both apparent power and power cost is computed. The apparent power device is linked with the watthour device, this linkage integrates the overall periodic procedure confirming maximum usage of the energy and resetting the necessary information to zero for respective periodic cycle (generally for each 15 to 30 minutes). The accuracy of KVA devices can be highly influenced by the harmonic’s currents occurred due to non-linear devices.

The induction motor theory underlies the operation of conventional watt-hour devices, in which the rotor element or revolving disk inside the meter spins at a speed associated with energy transfer. On the other hand, conventional magnetic watt-hour devices of the disc type usually demonstrate negative harmonic frequency discrepancies. That is, they might record lower energy levels at harmonic frequencies than at the basic frequency, whereas at higher frequencies, the decline is less pronounced.

Rectilinear devices include harmonic energy because of distorted voltage, but nonlinear devices typically inject harmonic energy back into the source model. Despite being utilized on a distorted electrical supply, measuring devices are calibrated on completely

sinusoidal alternating current. This results in a measuring inaccuracy. The amplitude and direction of the harmonic power determine the error sign. In contrast to producing torques, harmonic voltages or currents impair a meter's capacity to measure fundamental frequency power.

**VIII. Effect on Power System Protection**

Protective relays operational qualities are deteriorated by harmonics. The design parameters along with operating principles determine how harmonics affect the relay. Circuit breakers and fuse's ability to cause interruptions is impacted by current harmonic distortion. Due to more heating in the solenoid, harmonics cause increased di/dt at zero crossing point, and the thermal magnetic breakers' current detection capability modifies the trip point.

These downsides increase the cost of industrial manufacturing and other commercial events, due to the degrade seen in overall quality of the product material and decreased production [4].

**IX. Effect on Consumer Equipment**

Television Receivers: The change in picture size and brightness of the TV set is influenced by harmonics. Also, the amplitude modulation of the fundamental frequency is altered due to harmonics [4]. As, an example with introduction of 0.5% of inter-harmonic this leads to periodic amplification and decrement of the image of CRT screen.

In lighting systems like fluorescent and mercury arc lamps, capacitors combined with the inductive elements of the ballast and circuitry form a resonant network that produces a specific resonant frequency. This resonance can lead to excessive thermal stress, ultimately causing operational failure of the components. Additionally, harmonic voltage distortion contributes to the generation of audible noise, further impacting the system's performance and reliability.

### 2.4. Harmonic Analysis Techniques

Harmonic analysis involves measuring, modelling and assessing the impact of harmonics on power systems. Various techniques are used for harmonic analysis, including:

**I. Fourier Transform-Based Methods:**

This methodology is one of the versatile Frequency Domain Analysis that is employed for harmonics. The wide application of Digital Signal Processor and microcomputer have introduced the algorithms such as FFT and DFT [6]. These algorithms have accurate precision and can be employed to detect the selective order harmonics, but delay in a complete cycle is inevitable. Also, the actual meaning is not clear by the conversion between frequency and time domain.

It is the most powerful tool in mathematics, for converting a time-domain signal into the frequency domain

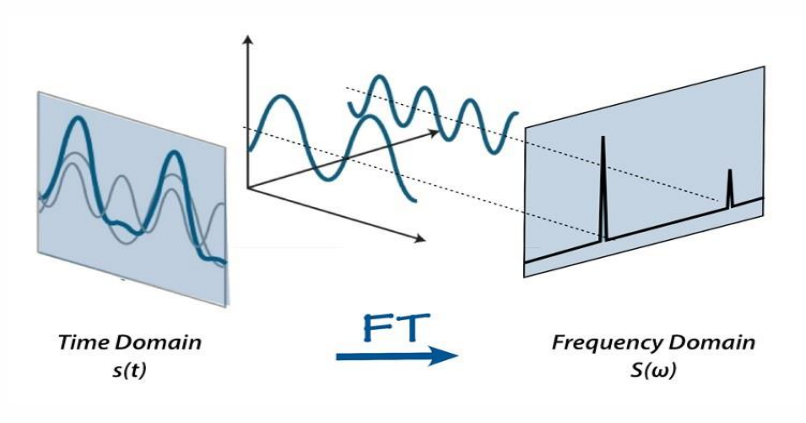


**Figure 2.1**:Conversion from time domain to frequency domain

For a continuous-time signal $f(t)$, the Fourier Transform $F\{f(t)\}$ is defined as [7]:

**II. Discrete Fourier Transform:**

Discrete signals are used in most instances of electrical parameter measurements. The Fourier transform (FT) is altered to switch from the Discrete Fourier transform (DFT) in order to handle such discrete signals.

For a sequence $x[n]$ of length $N$, where $n$=0,1,2,….,$N$−1, the DFT $X[k]$ is defined as [4]:

$$X[k] = \sum_{n=0}^{N-1} x[n]e^{-j\frac{2\pi}{N}kn}, k = 0,1, \dots, N-1 \quad \textbf{(2.1)}$$

where N represents the total number of samples within one period.

**III. Fast Fourier Transform (FFT)**

The primary disadvantage of DFT is that it takes considerable time to work out for big values of N. The Discrete Fourier transform can be computed effectively using FFT

technique. The matrix required for multiplication in the Discrete Fourier Transform (DFT) is decomposed into several simpler forms using the Fast Fourier Transform (FFT). This shortens both the execution time and the multiplication procedure [6].

**IV. Wavelet Transform (WT)**

It offers time-frequency localization, making it suitable for non-stationary harmonic analysis.

**V. Artificial Intelligence (AI) based methods**

Deep learning and machine learning techniques are increasingly applied for harmonic pattern recognition and classification.

**VI. MEMO-ESPRIT (Multiple Signal Classification and Estimation of Signal Parameters via Rotational Invariance Techniques)**

An advanced method for harmonic and inter-harmonic estimation with high resolution.

### 2.5. Types of filters

Filters are used in electrical and electronic systems to remove or reduce unwanted signals, such as harmonics in power systems or noise in communication systems. There are different types of filters according to their response characteristics. Some of them are:

#### 2.5.1 Passive Filter

They consist solely of passive components: resistors (R), inductors (L), and capacitors (C). They are simple, cost-effective, and reliable, but have fixed tuning and limited adaptability. Single-tuned filters are designed for a specific harmonic frequency. A High-Pass Filter allows higher frequencies while blocking lower ones. A Low-Pass Filter allows lower frequencies while blocking higher ones. A band-pass filter allows a specific range of frequencies to pass through while attenuating frequencies outside this range.

#### 2.5.2 Active Filter

They use power electronics and control algorithms to dynamically compensate for unwanted signals. An Active Power Filter (APF) is an electronic converter that generates and injects the required harmonic components into the system to cancel out the harmonics in the load current. Modern advancements in APF technology enable its

use for compensating reactive power, negative sequence currents, and harmonic currents.

A SAPF injects a compensating current to neutralize harmonics, while a Series Active Power Filter compensates for voltage harmonics by injecting a series voltage. Hybrid Active-Passive Filters combine passive filters with active components for better performance. The main goal of hybrid filters is to reduce the cost of static compensation. Passive filters are employed to cancel out the most significant harmonics of the load, while the active filter enhances the performance of the passive filters or cancels additional harmonic components. This approach reduces the power demand of the active filter and helps mitigate issues associated with passive filters, such as resonances with the source impedance.

**I.** Low-Pass Filter (LPF) permits low frequencies to pass through while attenuating higher frequencies.

**II.** High-Pass Filter (HPF) permits high frequencies to pass through while attenuating lower frequencies.

According to the literature, power filters are effective and commonly utilized solutions for limiting the spread of harmonic distortion in power systems Designing a passive power filter to effectively suppress harmonic current distortion caused by industrial nonlinear loads connected to a stiff power source presents a significant challenge. To enhance power quality, passive filters are typically integrated into the distribution system in both series and shunt configurations[8] . However, designing a passive power filter that effectively eliminates harmonic current distortion in industrial nonlinear loads connected to a rigid power source is a challenging task. Added to that, the passive filter has intrinsic disadvantages such instability, inflexibility, resonance with utility or load impedance, and massive bulk. On the other hand, in order to get around the negative aspects of the conventional filter, APFs that make use of VSIs have been explored as an alternative to passive filters. Active Power Filters (APFs) provide an ideal solution for power quality issues due to their numerous advantages, including flexibility, rapid dynamic response, and precise high-frequency filtering.

The massive size, resonance with utility or load impedance, instability, and stiffness of the passive filter are among its inherent disadvantages. To get around the drawbacks of

the conventional filter, APFs that use VSIs have been implied as an alternative to passive filters. APFs are the perfect answer for power quality issues because of its many attributes, which include flexibility, a quick dynamic response, and accurate ascendant filtering[8]. Active filter holds a major advantage over passive filter as these filters can be controlled to compensate the harmonics and the THD lesser than 5% can be efficiently attained at the point of common coupling.

Shunt APF adjusts for the harmonic currents induced by nonlinear loads by functioning as a current source. The control and the power circuit comprise a shunt active power filter, as illustrated in [9] . The compensating current is produced by the power circuit, which includes a DC-link capacitor for energy storage and DC voltage regulation, and a voltage source inverter (VSI) controlled through pulse-width modulation (PWM).
Additionally, the control circuit continuously tracks changes in harmonic currents to determine the instantaneous reference current required for compensation. It then uses this data to precisely control the power circuit, ensuring the delivery of the required harmonic current. The techniques utilized for harmonic extraction and current management have an immense effect on the overall efficacy of harmonic current compensation [7]. The operation of a shunt Active Power Filter (APF) relies on injecting a compensation current that is equal in magnitude but opposite in phase to the distorted current, thereby cancelling out the original distortion. In other words, the harmonic current injected by the shunt APF is 180° out of phase with the harmonic current drawn by the nonlinear load, resulting in the mutual cancellation of these components. This is achieved by "shaping" the compensation current waveform ($i_C$). The shape of the compensating current is determined by estimating the load current ($i_L$ ) and subtracting it from a sinusoidal reference [5]. The objective of the shunt Active Power Filter (APF) is to generate a sinusoidal source current ($i_s$) by utilizing the following relationship:

$$I_s = I_L - I_C \qquad \textbf{(2.2)}$$

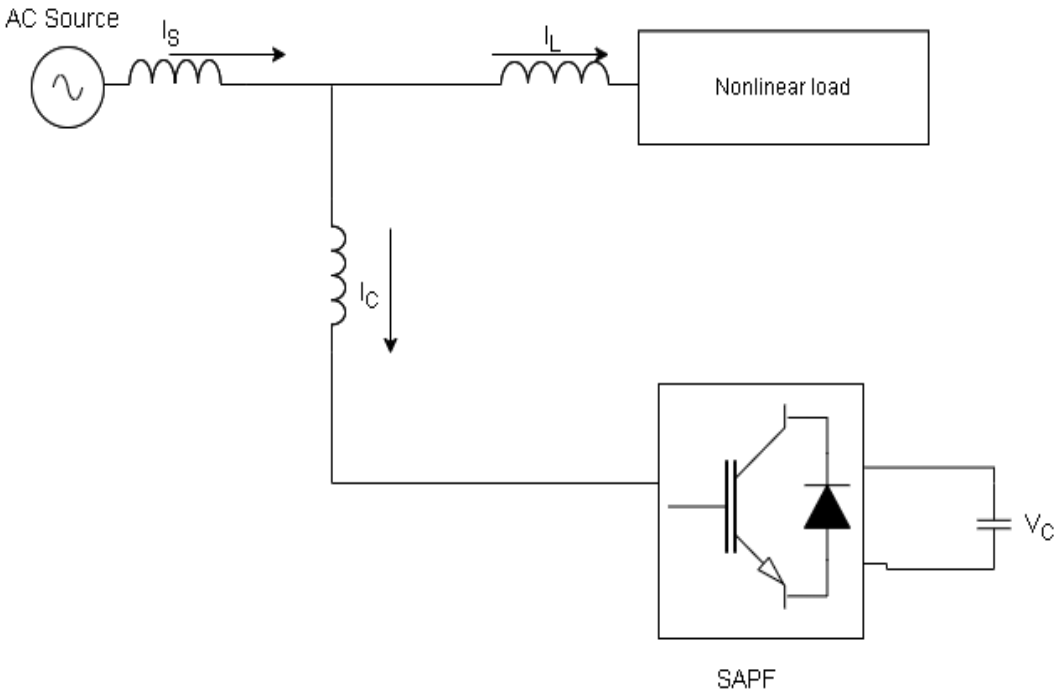


**Figure 2.2**:Circuit diagram of shunt active power filter

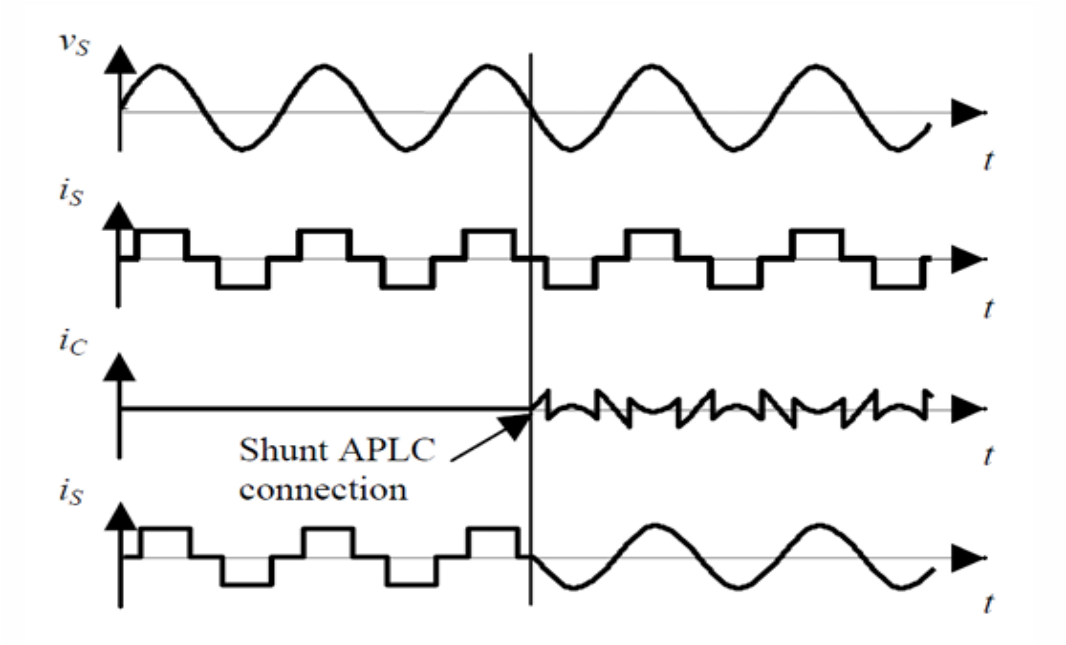


**Figure 2.3**: Waveform of source current after connecting filter

The effectiveness of a shunt active power filter in reducing harmonics is determined by the approach used for sensing current harmonics and reactive power, as well as the design and execution of the compensation control algorithm. These factors collectively determine the filter's ability to accurately identify and compensate for harmonic

distortions in the system [10]. The instantaneous reactive power theory is commonly adopted as the foundation for controlling compensation currents. The fundamental concept of this P–Q theory was originally coined by Akagi et al. in 1983[11].

Numerous scholars proposed a number of approaches to extract harmonic and fundamental components, including determining the reference compensation current and controlling the DC-link capacitor's voltage [10]. In [12], this paper author has utilized modified IRPT theory, which states that to govern the reference compensating current needed to eliminate harmonic currents caused by nonlinear loads connected at the point of common coupling (PCC). The study has shown that the harmonic proliferation across the feeder can be inhibited by an APF attached to the feeder's end bus. The outcomes pointed out that the suggested control method is capable of accounting for harmonic currents in both dynamic and steady-state load scenarios.

**III. Reference Frame Theory:**

In the abc-frame, the three axes are spaced 120 degrees apart to represent the three-phase current and voltage. The abc-reference frame is stationary, with the voltage and current in each phase following a sinusoidal waveform. The two axes, α and β, in the αβ-frame represent the exact balanced current and voltage. The β-domain is orthogonal to the α-domain, whereas the α-domain is equivalent to the a-axis of the conventional abc-domain. By reducing the number of necessary control loops, this transformation simplifies control in the αβ-frame by reducing the system from three axes to two.

The voltage or current components along the α and β axes continue to be sinusoidal over time in spite of this simplification. The 0 component in the αβ0 reference frame becomes zero in balanced systems, when the magnitudes of the α and β axes are equal. The α and β axes, on the other hand, become uneven in magnitude in imbalanced systems that contain negative and zero sequence components. This causes the 0 component within the αβ0 reference frame to have a non-zero value.

The Clarke transform is used to convert signals from the abc-frame to the αβ-frame. In a three-phase abc system, computations are more intricate and less intuitive. The Clarke transform simplifies this by offering a compact two-dimensional representation, which is well-suited for real-time digital control platforms such as DSPs and FPGAs. Since the αβ-frame is stationary, it is particularly advantageous in applications where tracking

a rotating reference frame isn't required, such as in vector motor control. This makes it an excellent choice for addressing THD mitigation in stationary, grid-tied systems.

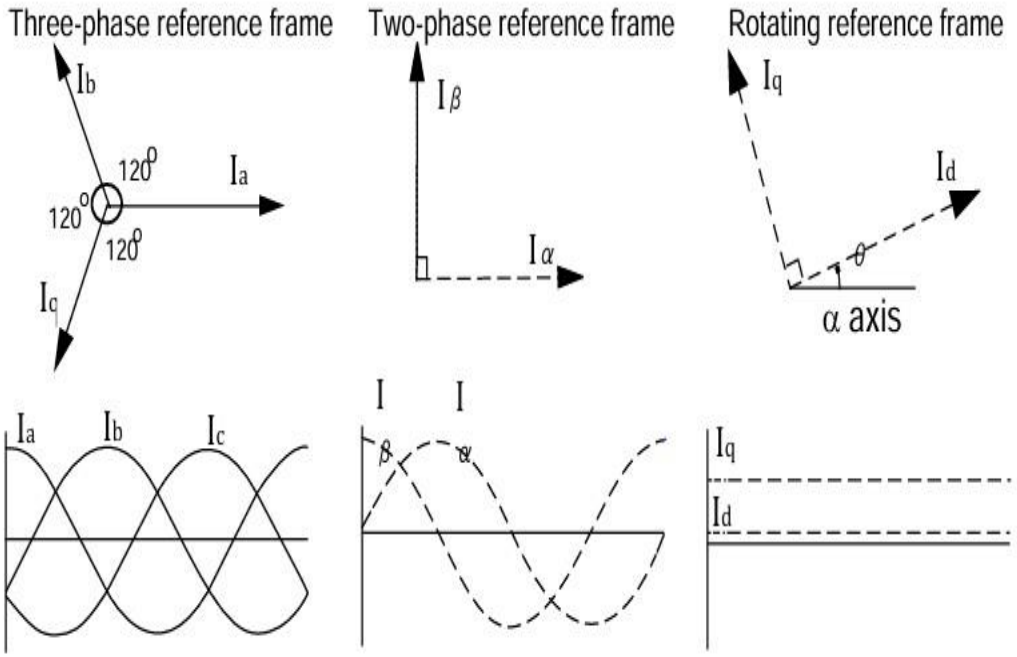


**Figure 2.4:** Currents in different reference frame

### 2.5.3 Harmonic Extraction:

The processes of harmonic extraction and estimation are essential in influencing the effectiveness and precision of a shunt active power filter utilizes various methods to determine the reference current, typically classified into two main categories: time-domain and frequency-domain approaches. The time-domain method is relatively straightforward, involving algebraic transformations and circuit-level analysis. It requires minimal computational resources, resulting in faster control operations. In contrast, the frequency-domain method is more complex, typically offering higher precision in harmonic compensation intricate and involves higher memory requirements due to its dependence on spectral analysis methods [6].

The instantaneous reactive power theory, commonly referred to as PQ theory, is formulated in the time domain and implemented through a simulation model developed in MATLAB/Simulink. At its core, IRPT involves transforming the stationary reference frame from the a-b-c coordinates to the 0-α-β coordinates a process referred to as the Clarke transformation. This coordinate transformation serves as the foundation for analysing and controlling power components in real-time. In Clark transformation, a

three-phase system is converted into a two-phase stationary reference frame. During this process, the voltage and current parameters are expressed as the sum of two mutually dependent and orthogonal vectors. These vectors simplify the analysis and control by providing a decoupled representation of the electrical quantities in the system. The representation of the Clark transformation is illustrated in the phasor diagram below:

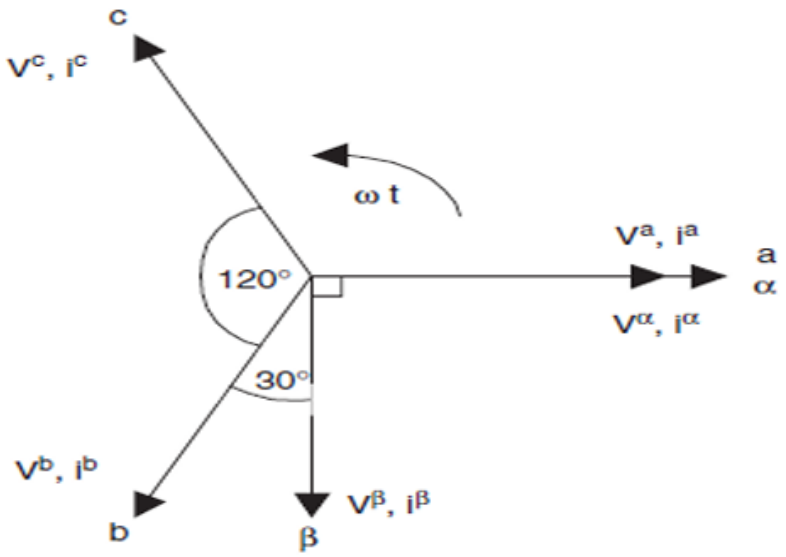


**Figure 2.5**: Reference currents in single phasor diagram

The conversion of source voltage and source current into 0-α-β components from abc components is as shown in the following expressions (2.3) and (2.4).

$$\begin{bmatrix} v_0 \\ v_\alpha \\ v_\beta \end{bmatrix} = \sqrt{\frac{2}{3}} \cdot \begin{bmatrix} 1/\sqrt{2} & 1/\sqrt{2} & 1/\sqrt{2} \\ 1 & -1/2 & -1/2 \\ 0 & \sqrt{3}/2 & \sqrt{3}/2 \end{bmatrix} \cdot \begin{bmatrix} v_a \\ v_b \\ v_c \end{bmatrix} \quad \textbf{(2.3)}$$

$$\begin{bmatrix} i_0 \\ i_\alpha \\ i_\beta \end{bmatrix} = \sqrt{\frac{2}{3}} \cdot \begin{bmatrix} 1/\sqrt{2} & 1/\sqrt{2} & 1/\sqrt{2} \\ 1 & -1/2 & -1/2 \\ 0 & \sqrt{3}/2 & \sqrt{3}/2 \end{bmatrix} \cdot \begin{bmatrix} i_a \\ i_b \\ i_c \end{bmatrix} \quad \textbf{(2.4)}$$

In the a-b-c coordinate system, the three-phase voltages are represented as $v_a$, $v_b$, and $v_c$, while the corresponding three-phase currents are denoted as $i_a$, $i_b$, and $i_c$. In the 0-α-β coordinate system, the voltages are indicated by $v_0$, vα, and vβ, and the currents are represented as $i_0$, iα, and iβ.

Total complex power is the sum of active power (p) and reactive power (q), which can be calculated using the following equation (2.5):

$$\begin{aligned} S = p + jq &= \boldsymbol{v}_{\alpha\beta}\boldsymbol{i}^*_{\alpha\beta} \\ &= \left(\boldsymbol{v}_\alpha - j\boldsymbol{v}_\beta\right)\left(\boldsymbol{i}^*_\alpha + j\boldsymbol{i}^*_\beta\right) \\ &= (\boldsymbol{v}_\alpha + \boldsymbol{v}_\beta\boldsymbol{i}_\beta) + j(\boldsymbol{v}_\alpha\boldsymbol{i}_\beta - \boldsymbol{v}_\beta\boldsymbol{i}_\alpha) \end{aligned} \quad \textbf{(2.5)}$$

Where, S represents the complex power, p is given by active power, q denotes the reactive power, and * characterizes the complex conjugate.

Hence, the instantaneous active and reactive power components in the α-β reference frame can be expressed in matrix form as follows:

$$\begin{bmatrix} p \\ q \end{bmatrix} = \begin{bmatrix} v_\alpha & v_\beta \\ -v_\beta & v_\alpha \end{bmatrix} \cdot \begin{bmatrix} i_\alpha \\ i_\beta \end{bmatrix} \quad \textbf{(2.6)}$$

In the presence of nonlinear loads, the instantaneous active and reactive powers are further divided into their DC and AC components. The DC component ($\overline{p}$) of the instantaneous active power represents the portion of power delivered from the source to the load and corresponds to the fundamental components of current and voltage. Conversely, the AC component reflects the exchange of energy between the source and the load (p*). A higher-order low-pass filter is employed to isolate the DC component of the instantaneous real power, which represents the portion of power that the three-phase AC source is required to supply[9]. The control schematic based on the Instantaneous Reactive Power Theory (IRPT) is illustrated in Figure 2.6.

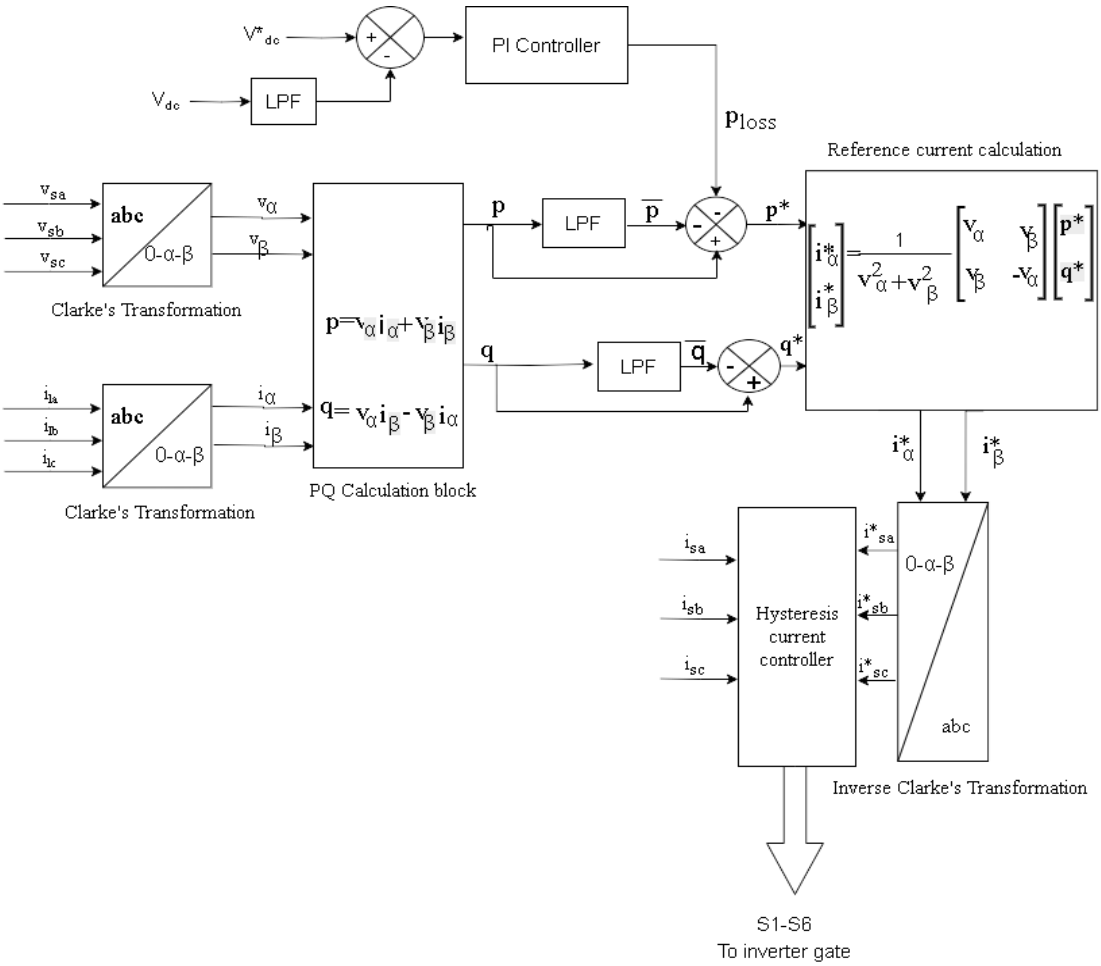


**Figure 2.6:** Instantaneous Reactive Power Theory Control Algorithm

Concerning about the instantaneous reactive power component ($Q$), $\bar{q}$ and q*, shows the fundamental and harmonic component respectively, that is responsible for the flow of energy between the load phases. The instantaneous current of α and β axis are given in equation below [13]:

α – axis instantaneous active current:

$$i_{\alpha p} = \frac{v_\alpha}{v_\alpha 2 + v_\beta 2} \cdot p \qquad \textbf{(2.7)}$$

α – axis instantaneous reactive current:

$$i_{\alpha q} = \frac{-v_\beta}{v_\alpha 2 + v_\beta 2} \cdot q \qquad \textbf{(2.8)}$$

β – axis instantaneous active current:

$$i_{\beta p} = \frac{v_\beta}{v_\alpha 2 + v_\beta 2} \cdot p \qquad \textbf{(2.9)}$$

β – axis instantaneous reactive current:

$i_{\beta q} = \frac{v_\alpha}{v_\alpha 2 + v_\beta 2} \cdot q$ **(2.10)**

$p = \bar{p} + p^*$ **(2.11)**

$q = \bar{q} + q^*$ **(2.12)**

The AC component (p*) of the active power and the total reactive power (q) are mandatory for the generation of harmonic reference currents. To compensate for the switching losses in the Voltage Source Inverter (VSI) and to maintain the DC-link voltage at the desired level, the SAPF needs a small amount of real power ($\bar{p}_{loss}$) from the three-phase AC source or an external power supply. Thus, the AC component (p*) of the active power can be computed by the given equation in (2.13):

$$p* = p - \bar{p} + \bar{p}_{loss} \quad \textbf{(2.13)}$$

$$\begin{bmatrix} i_a^* \\ i_\beta^* \end{bmatrix} = \frac{1}{v_\alpha^2 + v_\beta^2} \cdot \begin{bmatrix} v_\alpha & -v_\beta \\ v_\beta & v_\alpha \end{bmatrix} \cdot \begin{bmatrix} p* \\ q* \end{bmatrix} \quad \textbf{(2.14)}$$

$$\begin{bmatrix} i_a^* \\ i_b^* \\ i_c^* \end{bmatrix} = \sqrt{\frac{2}{3}} \cdot \begin{bmatrix} 1 & 0 \\ -1/2 & \sqrt{3}/2 \\ -1/2 & -\sqrt{3}/2 \end{bmatrix} \cdot \begin{bmatrix} i_\alpha^* \\ i_\beta^* \end{bmatrix} \quad \textbf{(2.15)}$$

Consequently, the compensating reference currents are first determined within the α-β coordinate system and then converted back to the a-b-c coordinate system through the application of the inverse Clarke transformation, as shown in the earlier expression. This procedure facilitates the application of reference currents in the three-phase system, thereby enabling efficient harmonic compensation.

### 2.5.4 Current Control Technique:

The establishment of appropriate criteria is a crucial step in the comparative analysis of different control mechanisms and the choice of a realistic test scenarios [14] to evaluate the performance level offered by each of the considered methods. In the overall design of the SAPF current control system, various control strategies are employed to generate the control pulses that dictate the switching behaviour of the filter. Among the different approaches, the hysteresis band current control method is widely adopted due to its simplicity and fast dynamic response in the following research for the generation of the

switching signals supplied to the VSI. The hysteresis current control method is widely used because of its straightforward implementation, high accuracy, rapid response, and robust stability[15], [16].

The main goal of using a current controller is to manage the load current, ensuring it follows the reference signal precisely. This is achieved by producing suitable switching signals for the inverter, keeping the current within a set hysteresis band, The load currents are constantly monitored and compared to their reference values through three separate hysteresis comparators. The results from these comparators are used to control the inverter's switching states [17]. Consequently, this method is widely favoured for its effectiveness. However, a notable drawback is the variation in the switching frequency throughout the fundamental cycle, which can lead to inconsistent inverter performance. To address this issue, several methods is suggested in the research to stabilize or minimize fluctuations in switching frequency.

Depending upon the hysteresis band configuration, current controllers are categorized into two types: the fixed-band and sinusoidal-band hysteresis current controllers. This classification is determined by the nature of the hysteresis band utilized in the control strategy. Figure. 2.7 and Figure. 2.8 illustrates the current waveforms for these controllers. In a sinusoidal band controller, the hysteresis band varies sinusoidally over a fundamental period, as shown in Figure. 2.7. The waveform of the fixed-band hysteresis current controller is shown in Figure. 2.8 [15].

In the fixed-band approach, the hysteresis band remains constant throughout the fundamental period. The mathematical model for this fixed-band scheme is expressed as follows:

$$I_{ref} = I_{max} \sin wt \quad \textbf{(2.16)}$$

$$I_{up} = I_{ref} + H \quad \textbf{(2.17)}$$

$$I_{low} = I_{ref} - H \quad \textbf{(2.18)}$$

In the above expressions $I_{up}$ refers to the upper band, $I_{low}$ is defined as the lower band, In the fixed-band scheme, H represents the hysteresis band limit. Referring to Figure 2.8, when $i_a > i_{up}$, the signal to the controller is 0, indicating that the inverter output voltage switches to negative to reduce the line current. Conversely, when $i_a < i_{low}$, the

signal is 1, causing the inverter output voltage to switch to positive to increase the line current.

In contrast, the sinusoidal-band scheme involves a hysteresis band that varies sinusoidally over the fundamental period [15] . Mathematical model of this scheme is given by the following equations:

$I_{ref} = I_{max}$ sinwt **(2.19)**

$I_{up} = (I_{max} + H)$ sinwt **(2.20)**

$I_{low} = (I_{max} - H)$ sinwt **(2.21)**

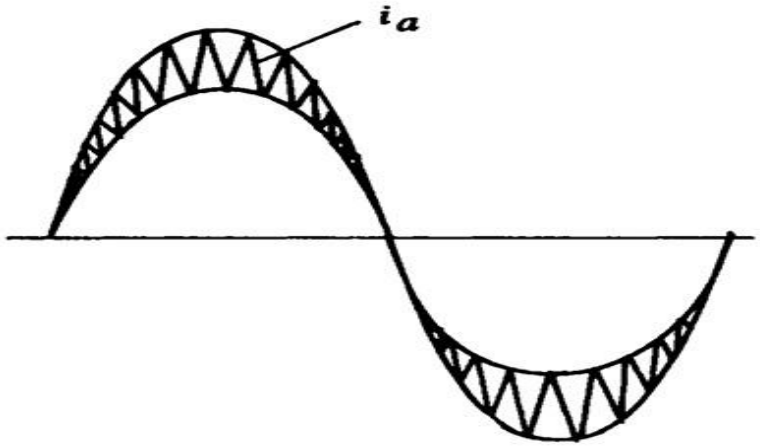


**Figure 2.7**: Hysteresis current controller waveform in sinusoidal frame

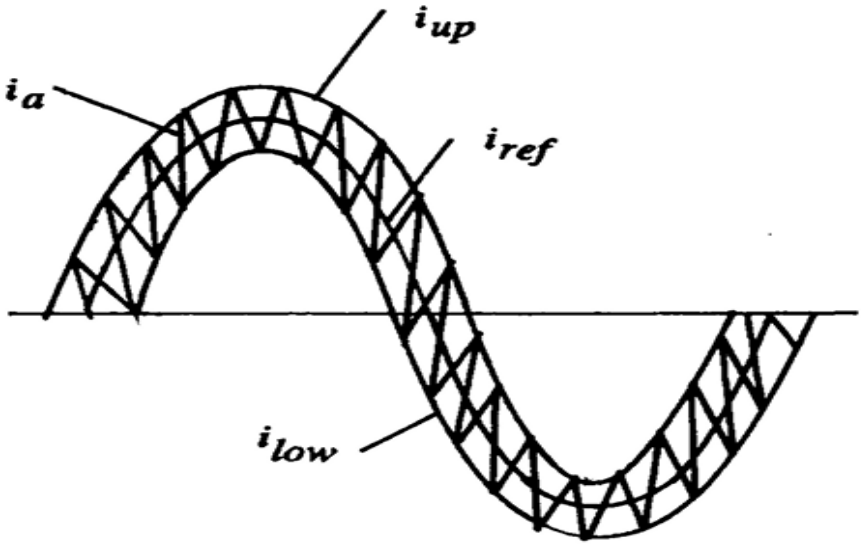


**Figure 2.8**: Hysteresis current band in fixed frame

The actual current ($i_{sa}$, $i_{sb}$, $i_{sc}$) and the reference current ($i_a$*, $i_b$*, $i_c$*) are compared to generate an error signal, which is then fed into the inverter. This causes the VSI switches to continuously turn on and off in order to keep the actual current within the hysteresis band. When the current error exceeds the upper threshold of the hysteresis band, the inverter adjusts accordingly, the output of the Voltage Source Inverter (VSI) is turned off, and conversely, it is turned on when the error drops below the lower limit. Generally, the DC voltage attains its peak value when there is a requirement to raise the output current, and drops to its lowest value when a reduction in current is necessary[9].

### 2.5.5 Proportional Integral (PI) Controller:

- Proportional (P) controller:

In a controller utilizing proportional control action, the relationship between the controller output m (manipulated variable) and the error signal e(deviation) is linear [18] .

Mathematically,

$m(t) = K_p\, e(t)$

After Laplace transformation,

$$M(s) = K_p\, E(s) \quad \textbf{(2.22)}$$

$$\text{or, } K_p = M(s)/E(s) \quad \textbf{(2.23)}$$

Where $K_p$ is recognized as proportional gain or proportional sensitivity.

- Integral Controller:

In a controller with integral control action, the controller output changes at a rate proportional to the integral of the actuating error signal e(t).

Mathematically,

$$\frac{d\, m(t)}{dt} = K_i\, e(t) \quad \textbf{(2.24)}$$

where, $K_i$ is a constant.

$$M(t) = K_i \int e(t) + m(0) \quad \textbf{(2.25)}$$

After Laplace transform,

$$sM(s) = K_i\, E(s) \quad \textbf{(2.26)}$$

$$\frac{M(s)}{E(s)} = \frac{K_i}{s} \quad \textbf{(2.27)}$$

Above equation (2.26) [18] is the transfer function of integral controller.

- **PI controller**

A Proportional-Integral (PI) Controller is a widely used control algorithm in power electronics, industrial automation, and motor drives. It is a type of closed-loop controller that improves system performance by adjusting the control input based on both the present and past errors[18].

The control output m(t) of a PI controller is given by:

$$m(t) = K_p e(t) + K_p K_i \int e(t)dt \quad \textbf{(2.28)}$$

$$\text{or, } m(t) = K_p e(t) + K_p \left(\frac{1}{T_i}\right) \int e(t)dt \quad \textbf{(2.29)}$$

Laplace transform,

$$M(s) = K_p E(s) + K_p / sT_i E(s) \quad \textbf{(2.30)}$$

$$M(s) = E(s) \left[1+\frac{1}{s\,Ti}\right] K_p \quad \textbf{(2.31)}$$

$$\frac{M(s)}{E(s)} = K_p\left[1+ \frac{1}{s\,Ti}\right] \quad \textbf{(2.32)}$$

where,

$K_p$ = Proportional gain (affects response speed and stability)

$K_i$ = Integral gain (eliminates steady-state error)

e(t)= Error signal

Another critical function of the SAPF is to regulate the DC-link voltage of VSI, ensuring it remains stable and within the desired range for efficient system performance. Typically, power filters that utilize VSIs for generation of harmonic reference currents include capacitor to store energy. In an ideal scenario, the voltage across the capacitor is same assuming there is no real power exchange between the filter and grid. However, during actual operation, the VSI draws small amount of real power to support its switching activity. To ensure a constant voltage and effective harmonic current compensation, a PI controller is incorporated into the control loop. In this scheme, the $V_{dc}$ is continuously compared against the $V_{dc\_ref}$, and resulting error signal.

PI controller processes a signal to eliminate steady-state errors in tracking the reference current.

The paper [19] further reviews studies on harmonics introduced by EV chargers and different compensation techniques. Researchers have proposed methods like estimation-based capacity calculation for SAPF sizing, active compensation, and advanced filtering techniques incorporating Kalman filters and sliding mode controllers. With the rise of EV adoption, the authors emphasize the importance of optimizing SAPF control strategies using intelligent algorithms to achieve better harmonic suppression. This study contributes by designing an optimal PI controller for SAPF using a Criminal Search Optimization Algorithm (CSOA), which enhances DC-link voltage regulation and improves power quality in EV charging stations. The proposed method is validated through MATLAB/Simulink simulations and real-time implementation using an OPAL-RT simulator, demonstrating its effectiveness compared to conventional optimization techniques like PSO, WOA, ACO, and BCO.

The author of paper[20] contributes to the field by proposing an analytical model for estimating SAPF capacity based on harmonic parameter estimation and analytical modelling, validated through simulation and real-world testing in an EV charging station. The authors analyse the operational principles of a three-phase uncontrolled rectifier charger in both continuous conduction mode (CCM) and discontinuous conduction mode (DCM). They propose a parameter estimation method for the equivalent circuit of EV chargers using measured AC voltage and current waveforms. The estimation focuses on key circuit parameters, including DC voltage, filter inductance, and load resistance, using mathematical models based on conduction angle analysis.

Researchers have developed both DC and AC charging pile circuit models[21], which helps in analysing the electrical characteristics of charging infrastructure. These models have been instrumental in examining the harmonic distortion effects caused by EV chargers, particularly in the context of rectification and power conversion processes. Additionally, this paper has focused on the noise generated by charging piles, investigating both conducted and radiated electromagnetic interference (EMI) to assess their impact on the power system and surrounding equipment.

From paper[22] , a comprehensive analysis of harmonic emissions resulting from the smart charging of electric vehicles (EVs) is presented. This research encompasses eight distinct EV models, reflecting the current market's diversity by considering various aspects such as vehicle age, battery capacity, and the type of onboard charging systems—whether integrated or dedicated. The harmonic emission data were evaluated based on amplitude, phase angle, and total harmonic distortion, with particular attention to current (THDI) and voltage (THDV) distortions. The results reveal that EVs charged at lower smart charging current setpoints tend to generate higher harmonic distortions, as evidenced by increased THDI values. Among the studied models, the Peugeot e-2008 recorded the highest THDI, ranging from 11% to 26%. Furthermore, the Tesla Model Y Long Range and two versions of the Renault Zoe displayed similar magnitudes of individual harmonic distortion components.

The findings of paper[22] highlights the significance of harmonics-aware smart charging strategies that not only support demand-side management but also help in reducing harmonic distortion. Moreover, the study underlines the necessity for developing more sophisticated probabilistic models capable of evaluating and minimizing harmonic impacts in practical scenarios, considering both electric vehicles and other non-linear loads connected to the same PCC. These crucial findings lay a solid foundation for future research aimed at enhancing existing standards to accommodate the increasing integration of EVs into modern electrical grids.

In the paper[23], with significant reference to the limited experimental data available, which consists of fewer than a dozen studies from the past decade, the typical emission mechanisms, spectral behaviour, and the superposition of emissions from various chargers, along with the existing LV grid distortion, were discussed. Harmonic distortion remains highly variable across different electric vehicle (EV) models and, in certain conditions, can exceed the permissible limits set by IEC standards, despite the widespread implementation of power factor correction (PFC) techniques. The superposition of harmonics is further complicated by the presence of various distorting loads—such as residential and office appliances, which have a significant presence within the AC grid. Notably, certain dominant low-order harmonics demonstrate sensitivity to the waveform of the grid voltage, particularly under conditions where flat-top voltage profiles, often influenced by third harmonic contamination, are present.

This underscores the importance of conducting harmonic emission assessments under conditions that closely replicate real-world usage. Within the supraharmonic frequency range, emissions originating from the PFC stage and downstream power converters within the EV are observed, typically manifesting as a primary switching frequency and its associated harmonics. Additionally, broadband emissions may be detected in the lower frequency range, typically below 10 kHz, driven by impulses generated from the PFC operation[23].

### 2.5.6 IEEE Standard for Harmonics:

To limit the harmonic currents into the power system, IEEE Standards Association has established guidelines and limitations regarding harmonic standards (IEEE Std 519-1992 [24]), which was further refined in 2014 (IEEE Std 519–2014). From this standard the THD shall not exceed 5%[24]. This work explores various sources of harmonics, including VAR compensators, cyclo-converters, switch-mode power supplies, pulse-width modulated drives, inverters used in distributed generation, and waveform distortion caused by harmonics. It also analyses distortions in low-voltage distribution feeders, industrial networks, and transmission systems. Furthermore, it addresses the impact of harmonic distortion on the performance of several devices or loads such as motors, generators, transformers, power cables, capacitors, and electronic equipment is discussed. As a result, power filters are utilized to ensure compliance with the 5% harmonic distortion limit.

# CHAPTER 3: METHODOLOGY

This chapter describes the method, tools, and techniques used, starting with data collection from the feeder and charging station, and their detailed modelling for harmonic analysis of the charging station on the distribution network.

### 3.1.1 Approach

Initially, a literature review is conducted to understand the concepts of harmonic analysis, the impacts of harmonics on low-voltage distribution networks, the need for harmonic analysis, and possible mitigation methods. The required data is then collected from the Pulchowk DCS for the modelling of the Sanepa feeder and Sajha Yatayat. Figure.3.1 outlines a structured process for analysing and mitigating harmonic distortion in an electrical feeder with an EV charging station using MATLAB/Simulink. The process begins with a literature review to understand power quality, harmonic distortion, and mitigation techniques. Next essential data, including (i.e. transformer specifications, line length, load details and charger characteristics) were collected to build an accurate system model. A simulation model is developed in MATLAB/Simulink, which includes the grid, feeder, and charging station. The simulation is executed to analyse the harmonic distortion. The THD is then compared with IEEE standards to determine compliance. If THD exceeds acceptable limits, a SAPF is designed and integrated into the model to mitigate harmonics. After implementing the filter, the simulation is re-run, and the model results are analysed to verify the reduction in THD. Finally, the entire process, including data collection, simulation setup, THD analysis and SAPF performance evaluation is thoroughly documented for validation.

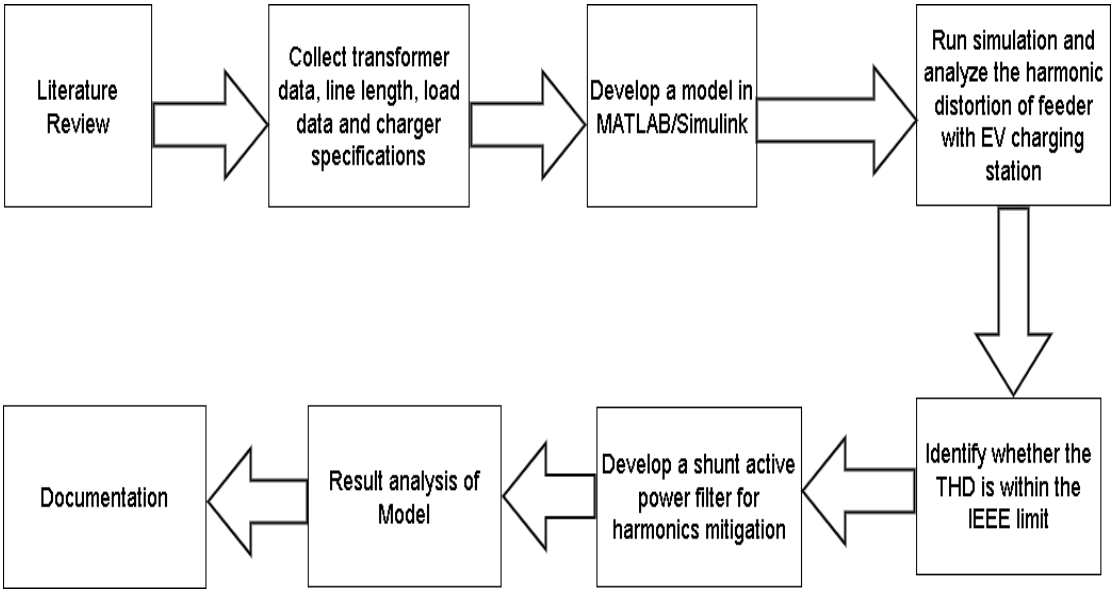


**Figure 3.1**: Flowchart of the approached methodology

### 3.1.2 Data Collection

The EV charging stations are to be provided with a 3-phase, 400V, 50Hz AC supply through the distribution transformers connected an 11kV feeder line as per the NEA specifications. This work conducts the study of total harmonic distortion on the Sanepa distribution feeder of Kathmandu valley due to an electric vehicle charging station. The feeder is supplied by Thapathali Switching Station. This feeder consists of 20 transformers, and the feeder length is 9.6km. This 11kV system consists of commercial as well as residential loads. Figure. 3.2 shows a GIS map view:

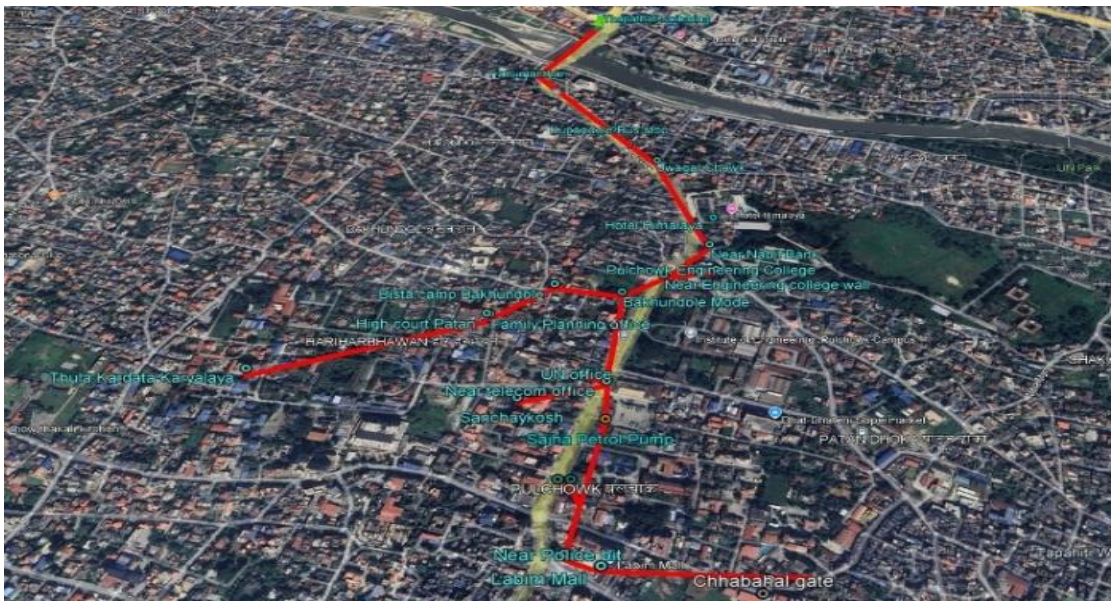


**Figure 3.2**: GIS map view of Sanepa Feeder

### 3.1.3 System Modelling

The feeder is modelled in the MATLAB/Simulink environment. Initially, the model was developed to analyse the system behaviour before the sajha charging station was integrated and the THD in the grid was evaluated. Subsequently, a charging station load was incorporated at the feeder and THD analysis was performed. To mitigate the harmonic distortion introduced due to charging station, a SAPF is designed and connected in parallel. The input voltage for the charger is 380V AC with a tolerance of ±15%. The output voltage varies between 200 and 750V DC while the maximum output current is 150A DC. The charger has an output power of 90KW. The rated frequency ranges from 45Hz to 65Hz data which is shown in Table. 3.1

**Table 3.1: Charger Specifications**

| **Charger Specifications** | |
|---|---|
| Input Voltage | 380V±15% AC |
| Input Current | 131A AC max |
| Rated frequency | 45-65 Hz |
| Output Voltage | 200 ~750V DC |
| Output Current | 150A DC max |
| Output Power | 90KW |
| Ambient Temperature | -30◦C ~ +55◦C |

Table. 3.2 specifies the electrical characteristics of the power system. The main source voltage is 11kV. A transformer with a rating of 11kV/0.4kV is used to step down the voltage from 11kV to 400V for load-side applications. The load-side AC voltage is maintained at 400V which is suitable for EV charging station. The system frequency is 50Hz. An AC inductor of 1.5mH is included, which helps in filtering harmonics current flow. The power electronic converters or filters in the system operate at the switching frequency of 10kHz.

**Table 3.2: Feeder and filter data**

| Parameter Details | |
|---|---|
| Main source voltage | 11kV |
| System Frequency | 50Hz |
| Transformer | 11/0.4kV |
| Load side ac voltage | 400V |
| Ac inductor | 1.5mH |
| Switching Frequency | 10KHz |
| $K_p$ | 1.2 |
| $K_i$ | 8 |
| $C_{dc}$ | 1000 micro-farad |

### 3.1.4 Tools and Software

The technical and scientific advancements in the field of computer architecture, software, and various programming tools have made the modelling and study of power systems easier. In the past, modelling and analysis were tough, time-consuming, and less accurate due to slow processing tools and software. In this section, the tools used to carry out this dissertation are listed.

**I. Microsoft Office**

Microsoft Office or MS Office, is a suite of desktop productivity applications developed by Microsoft. It contains Microsoft Word, Microsoft Excel, and Microsoft PowerPoint as the core products. In this study, Microsoft Word is used as documentation of the task, and Microsoft Excel is used for managing data and performing calculations.

**II. MATLAB**

MATLAB, short for MATrix LABoratory, is a proprietary multi-paradigm programming language and numerical computing environment developed by MathWorks. It enables matrix manipulation, function and data plotting, algorithm implementation, user interface creation, and integration with programs written in other

languages. In this work, MATLAB/Simulink is used for the modelling of basic power system network consisting of a voltage source, distribution line impedance, and a nonlinear load. To mimic a realistic scenario, an electric vehicle (EV) charging station was integrated at the distribution feeder. Also, a SAPF using a current controlled voltage source converter (VSC) to compensate for the harmonic currents generated by the charging station was designed in Simulink environment. Throughout the simulation process Fast Fourier Transform (FFT) blocks were used to measure THD, and scopes were employed to visualize voltage and current waveforms. Figure. 3.3 shows the overall diagram of the system containing source, line impedance and active power filter:

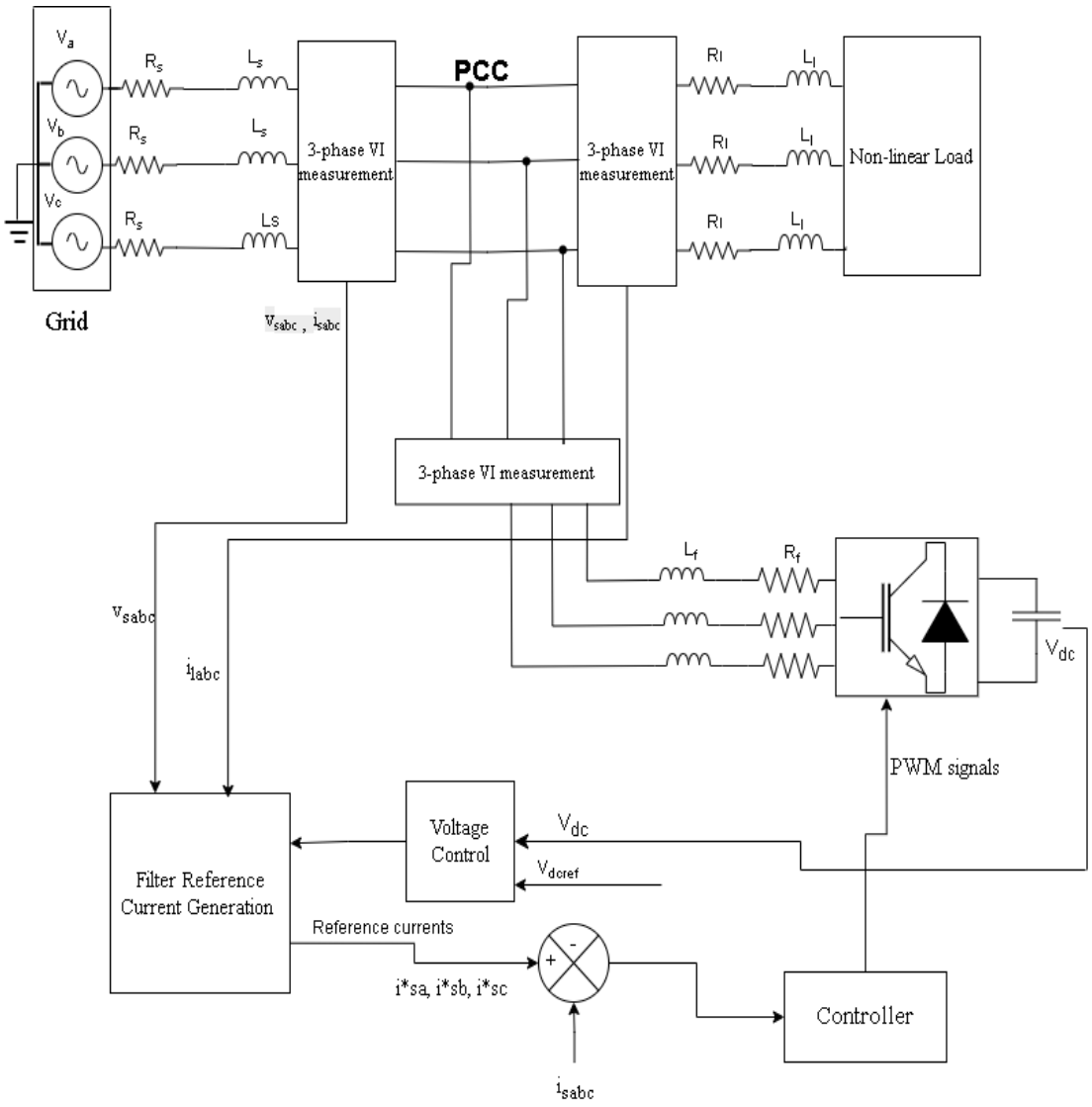


**Figure 3.3**: Overall System Diagram

# CHAPTER 4: RESULTS AND DISCUSSION

At first, the system was tested for the condition before the charging station was integrated. Sanepa feeder is in an urban area where a lot of other commercial buildings and nonlinear loads are also present.

For the charging station, an 11/0.4 kV transformer is used to step down the voltage. The source voltage waveform is shown in Figure. 4.1:

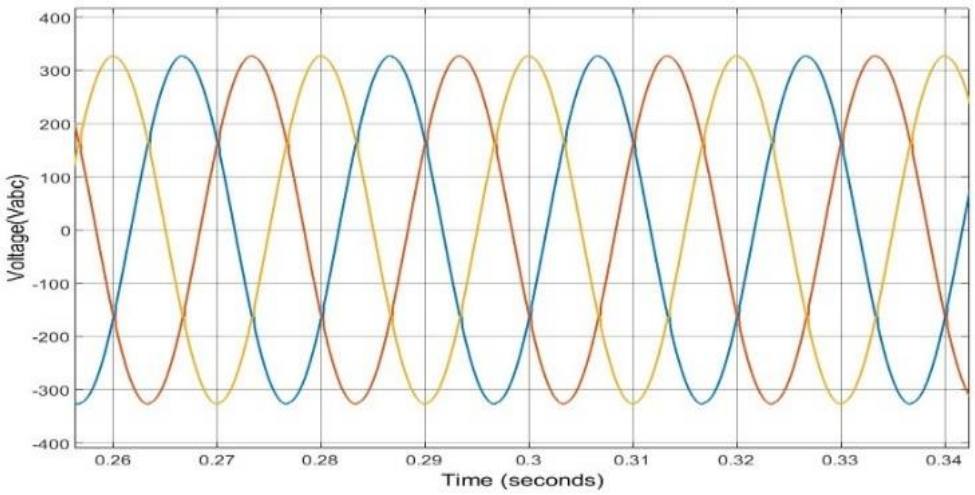


**Figure 4.1**: Waveform of source voltage

After connecting the charging station to the system, the presence of power electronic converters further distorted the current compared to original current. Figure. 4.2 and Figure. 4.3 shows the waveforms for distortion of three-phase load and source currents:

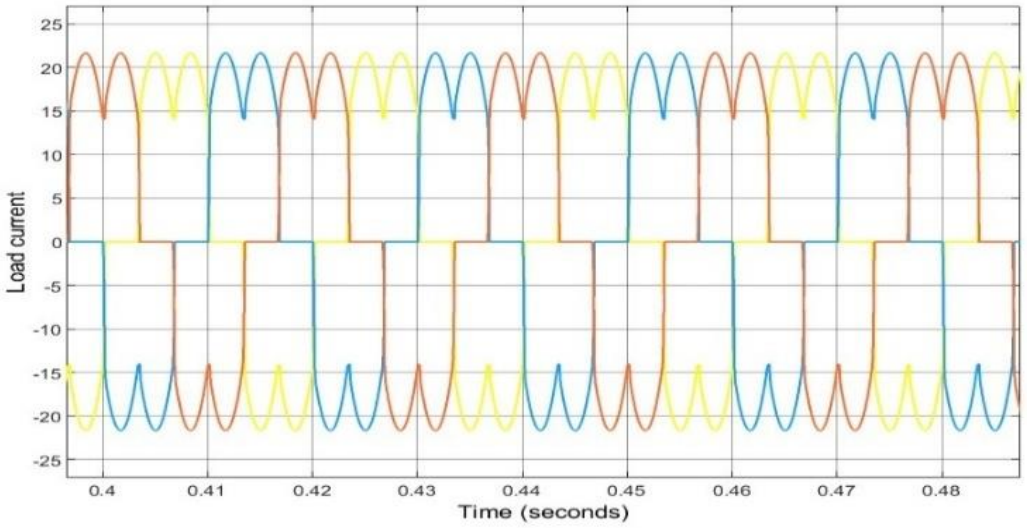


**Figure 4.2**: Waveform of load current after connecting charging station

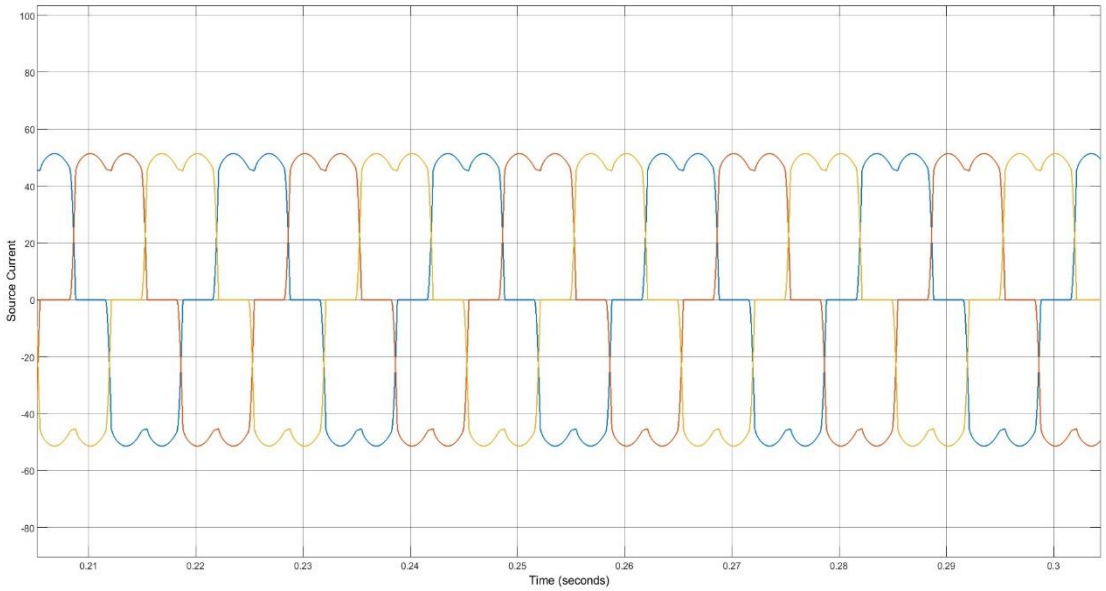


**Figure 4.3**: Waveform of source current after connecting charging station

The Figure. 4.4 describes about the compensated source current of phase "a" after connecting the SAPF. The filter supplied the compensating harmonic current equal to the distorted current, resulting in a sinusoidal waveform.

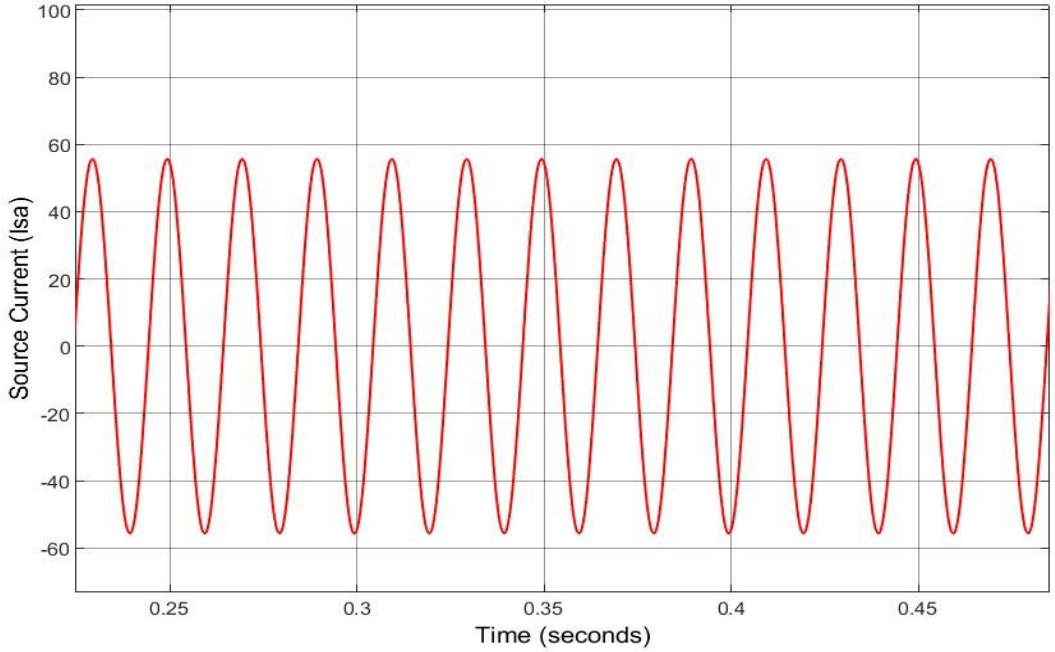


**Figure 4.4**: Compensated source current of phase a after connecting filter

There is a distortion in source current due to presence of the nonlinearity behaviour of the charging stations, which contain AC-DC rectifier for converting the utility source voltage to DC form and dc-dc converter for buck/boost the voltage level according to the battery. Figure. 4.5 depicts the FFT analysis for the total harmonic distortion of the source current as 27.31%, which surpasses the IEEE harmonic standard limit. The dominant harmonics are $5^{th}$ ,$7^{th}$ ,$11^{th}$ ,$13^{th}$ and $17^{th}$ respectively**.**

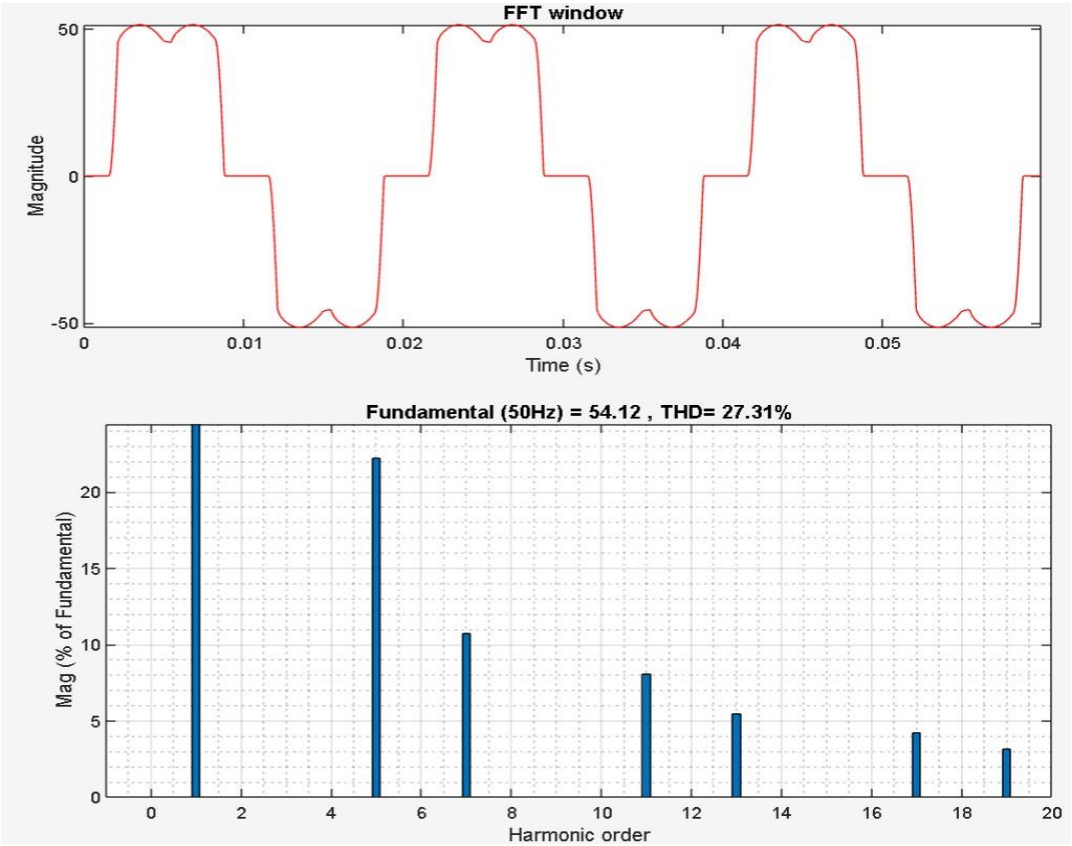


**Figure 4.5**: FFT analysis of source current before compensation

The THD of the system exceeds the IEEE limit, and to mitigate this, a shunt active power filter is connected at the point of common coupling. The instantaneous reactive power theory control algorithm is used to provide the reference current equal to the harmonic current to make the source current more sinusoidal. Figure.4.6 portrays a Simulink model of the reference compensation current generation (I*a, I*b, and I*c) in a-b-c frame, respectively.

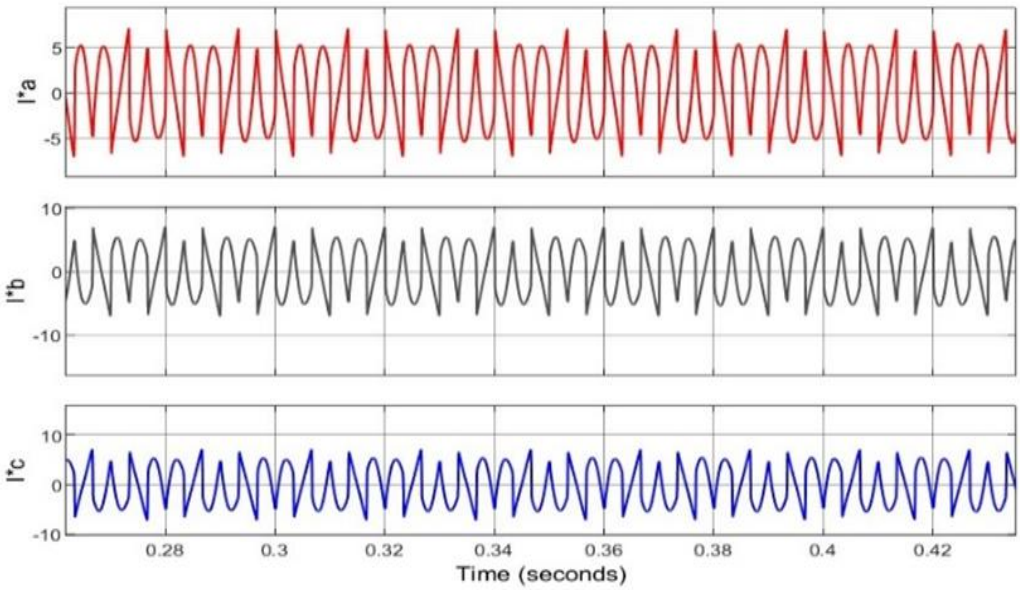


**Figure 4.6**: Transformed reference currents in abc frame

Figure. 4.7 shows the THD of the system after connecting the shunt active power filter at the point of common coupling. It reduces the total harmonic distortion to 1.23% from 27.31% which is within the grid code[25] IEEE limit.

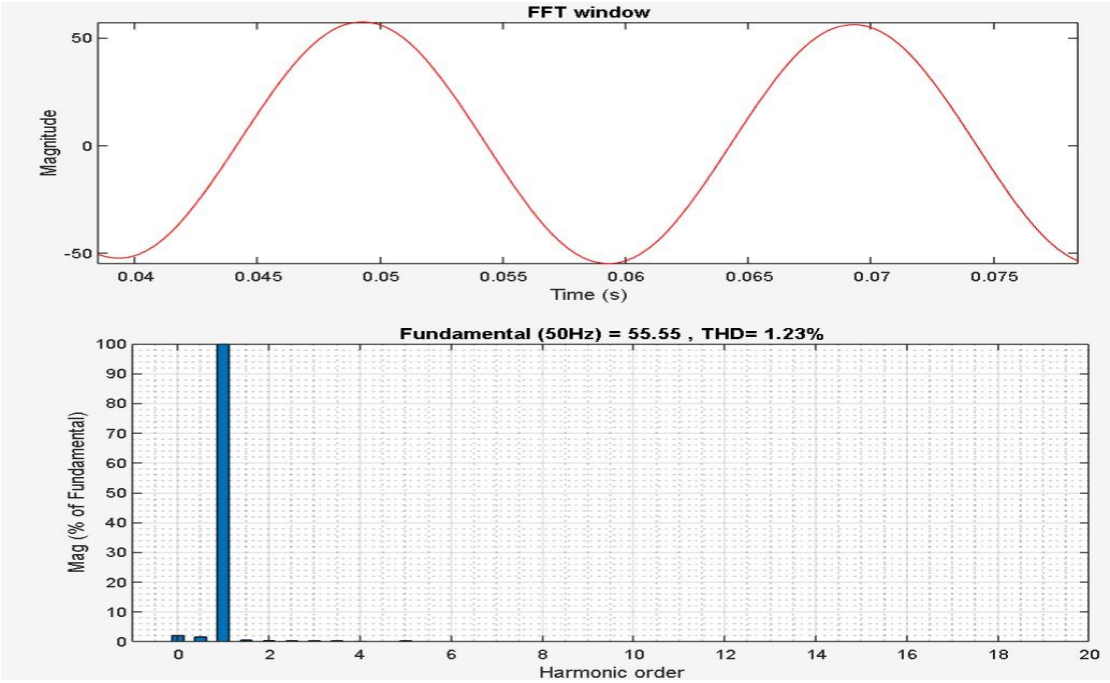


**Figure 4.7**: Source current FFT analysis after compensation

After the reduction of the THD of the system, the source current becomes sinusoidal, which is illustrated in Figure. 4.4.

# CHAPTER 5: CONCLUSION AND RECOMMENDATIONS

There is an increasing trend of electric vehicles globally as well as in Nepali automotive industry. In this study, a model of a Sanepa distribution feeder is developed where there are charging stations located. Involvement of power electronics converters in charging topology acts as a non-linear load that actively brings distortion in the current and voltage waveforms. The simulation results demonstrate that integrating charging stations on a large scale significantly injects harmonic currents, distorting the current waveform. On doing the Fast Fourier Transform analysis before compensation, as shown in Figure. 4.7, the total harmonic distortion rose to 27.31% in the form of different scales of harmonics, which is much higher than the IEEE limit. The shunt active power filter proposed in this paper is a viable solution to compensate for such distortion present in the system. After the use of the filter, the total harmonic distortion was reduced to 1.23%. This suggests that the use of a shunt active power filter provides superior performance, compensating for harmonics in real-time and ensuring compliance with IEEE 519 standards.

Future works shall focus on techno-economic assessment of SAPFs by making advancements in control algorithms. As smart grids are becoming more prevalent, the application of SAPFs in real-time harmonic mitigation and how they can communicate with other smart grid elements to ensure power quality shall be further explored. The harmonics produced by power electronics converters are characterized by high frequency, a broad frequency range, and multi-type coupling. Additional research is needed to develop methods for identifying and suppressing high-order harmonics and inter-harmonics.

## REFERENCES


[1] Zhiyun Li, "A Review of the Current Status of Global Electric Vehicle Charging Infrastructure Development," *Internation journal of Global Economics and Management*, vol. 3, 2024.

[2] P. Biswas *et al.*, "Vehicle to Grid: Technology, Charging Station, Power Transmission, Communication Standards, Techno-Economic Analysis, Challenges, and Recommendations," Mar. 01, 2025, *Multidisciplinary Digital Publishing Institute (MDPI)*. doi: 10.3390/wevj16030142.

[3] J. Su, T. T. Lie, and R. Zamora, "Integration of Electric Vehicles in Distribution Network Considering Dynamic Power Imbalance Issue," *IEEE Trans Ind Appl*, vol. 56, no. 5, pp. 5913–5923, Sep. 2020, doi: 10.1109/TIA.2020.2990106.

[4] E. F. and M. M. A. Fuchs, *POWER QUALITY IN POWER SYSTEMS AND ELECTRICAL MACHINES*. Academic press, 2011.

[5] "IEEE Standard for Shunt Power Capacitors," *IEEE Std 18-2002 (Revision of IEEE Std 18-1992)*, pp. 1–20, 2002.

[6] H. Li, F. Zhuo, Z. Wang, W. Lei, and L. Wu, "A novel time-domain current-detection algorithm for shunt active power filters," *IEEE Transactions on Power Systems*, vol. 20, no. 2, pp. 644–651, May 2005, doi: 10.1109/TPWRS.2005.846215.

[7] Sabir Ouchen and Jean-Paul Gaubert and Heinrich Steinhart and Achour Betka, "Energy quality improvement of three-phase shunt active power filter under different voltage conditions based on predictive direct power control with disturbance rejection principle," *Math Comput Simul*, vol. 158, no. 0378–4754, pp. 506–519, 2019.

[8] Z. Salam, A. Jusoh, and T. P. Cheng, "Harmonics mitigation using active power filter: A technological review," 2006. [Online]. Available: https://www.researchgate.net/publication/41057887

[9] A. A. Imam, R. Sreerama Kumar, and Y. A. Al-Turki, "Modeling and simulation of a pi controlled shunt active power filter for power quality enhancement based on p-q theory," *Electronics (Switzerland)*, vol. 9, no. 4, Apr. 2020, doi: 10.3390/electronics9040637.

[10] M. Y. and M. V. and P. S. and C. V. and S. I. Artemenko, "Modified Instantaneous Power Theory for Three-Phase Four-Wire Power Systems ," *2019*

*IEEE 39th International Conference on Electronics and Nanotechnology (ELNANO)*, pp. 600–605, 2019.

[11] Y. K. K. F. A. N. Hirofumi Akagi, "Generalized theory of instantaneous reactive power and its application," 1983.

[12] *2019 IEEE 39th International Conference on Electronics and Nanotechnology (ELNANO) : conference proceedings : April 16-18, 2019, Kyiv, Ukraine*. IEEE, 2019.

[13] H. Akagi, Y. Kanazawa, and A. Nabae, "Instantaneous Reactive Power Compensators Comprising Switching Devices without Energy Storage Components," *IEEE Trans Ind Appl*, vol. 20, no. 3.

[14] S. Buso, L. Malesani, and P. Mattavelli, "Comparison of Current Control Techniques for Active Filter Applications," *IEEE TRANSACTIONS ON INDUSTRIAL ELECTRONICS*, vol. 45, no. 5, 1998.

[15] M. A. Rahman, T. S. Radwan, A. M. Osheiba, and A. E. Lashine, "Analysis of Current Controllers for Voltage-Source Inverter," *IEEE TRANSACTIONS ON INDUSTRIAL ELECTRONICS*, vol. 44, no. 4, p. 477, 1997.

[16] H. Mao, X. Yang, Z. Chen, and Z. Wang, "A hysteresis current controller for single-phase three-level voltage source inverters," *IEEE Trans Power Electron*, vol. 27, no. 7, pp. 3330–3339, 2012, doi: 10.1109/TPEL.2011.2181419.

[17] K. M. Rahman, M. Rezwan Khan, M. A. Choudhury, and M. A. Rahman, "Variable-Band Hysteresis Current Controllers for PWM Voltage-Source Inverters," *IEEE Trans Power Electron*, vol. 12, no. 6, 1997.

[18] S. H. Saeed, *Automatic Control System*, Revised. S. K. Kataria & Sons, 2008.

[19] A. Srivastava and S. Saravanan, "Harmonic mitigation using optimal active power filter for the improvement of power quality for a electric vehicle changing station," *e-Prime - Advances in Electrical Engineering, Electronics and Energy*, vol. 8, Jun. 2024, doi: 10.1016/j.prime.2024.100527.

[20] N. Zhou, J. Wang, Q. Wang, N. Wei, and X. Lou, "Capacity calculation of shunt active power filters for electric vehicle charging stations based on harmonic parameter estimation and analytical modeling," *Energies (Basel)*, vol. 7, no. 8, pp. 5425–5443, 2014, doi: 10.3390/en7085425.

[21] Y. and Y. D. and Z. G. and W. H. and Z. J. Zhang, "Harmonic Analysis of EV Charging Station Based on Measured Data," *2020 IEEE/IAS Industrial and Commercial Power System Asia (I&CPS Asia)*, pp. 475–480, 2020.

[22] M. Senol *et al.*, “Harmonics Measurement, Analysis, and Impact Assessment of Multiple Electric Vehicle Smart Charging,” *IEEE Open Journal of Vehicular Technology*, 2024, doi: 10.1109/OJVT.2024.3505778.

[23] A. Mariscotti, “Harmonic and Supraharmonic Emissions of Plug-In Electric Vehicle Chargers,” *Smart Cities*, vol. 5, no. 2, pp. 496–521, Jun. 2022, doi: 10.3390/smartcities5020027.

[24] D. Committee of the IEEE Power and E. Society, “IEEE Recommended Practice and Requirements for Harmonic Control in Electric Power Systems Sponsored by the Transmission and Distribution Committee IEEE Power and Energy Society.”

[25] C. K. and S. R. P. Duffey, “Update of harmonic standard IEEE-519: IEEE recommended practices and requirements for harmonic control in electric power systems,” *IEEE Trans Ind Appl*, vol. 25, pp. 1025–1034, 1989.

## APPENDIX A: SIMULATION DIAGRAMS

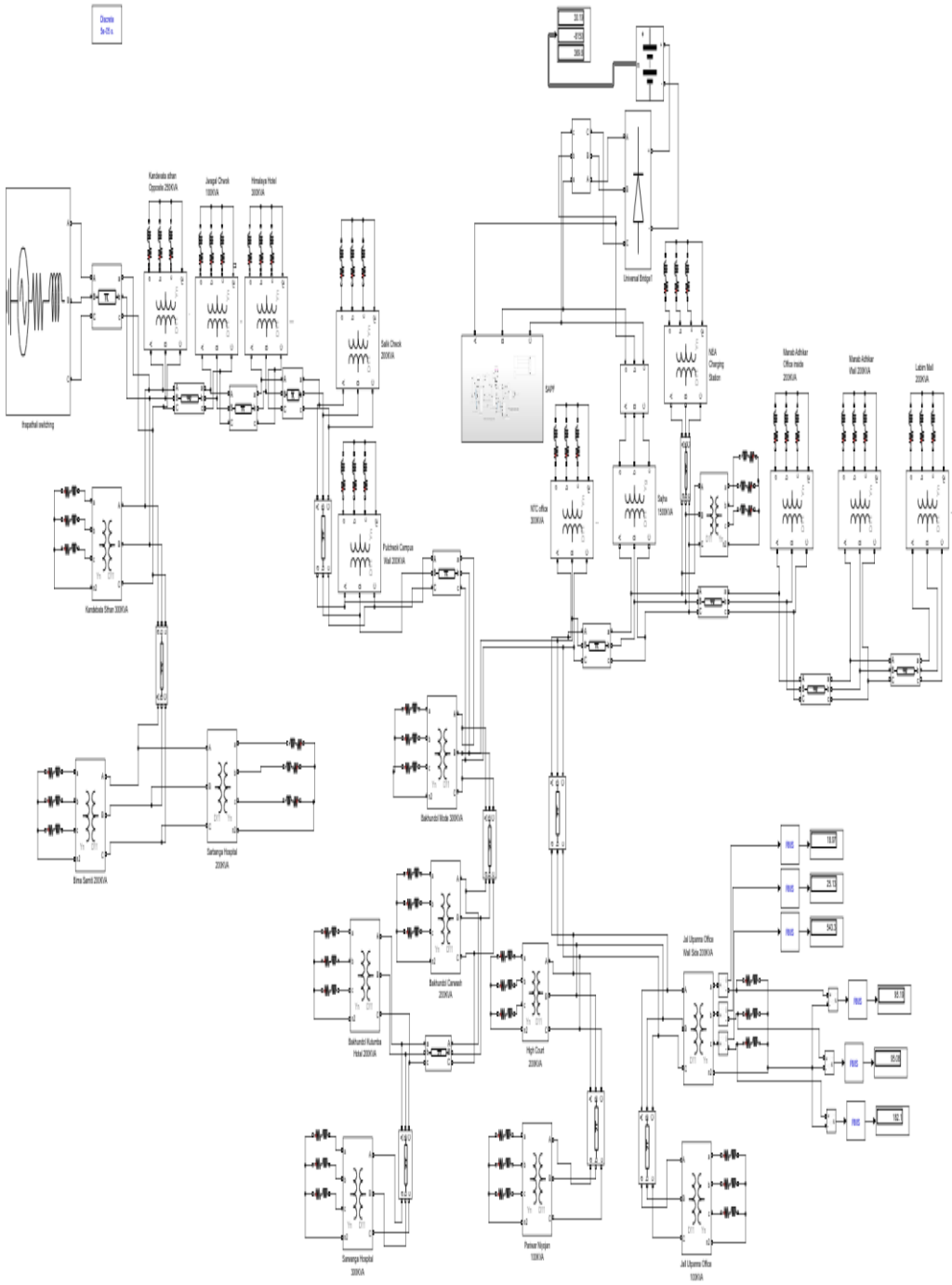

Figure: Overall simulation diagram of the feeder

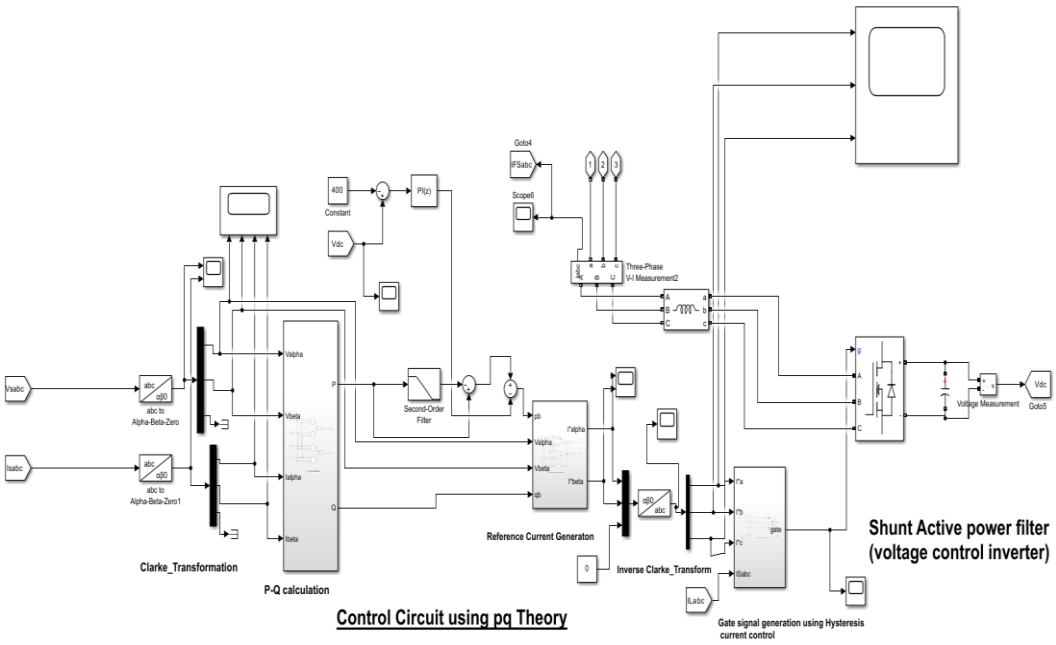


Figure: Simulation Diagram of Instantaneous Reactive Power Theory

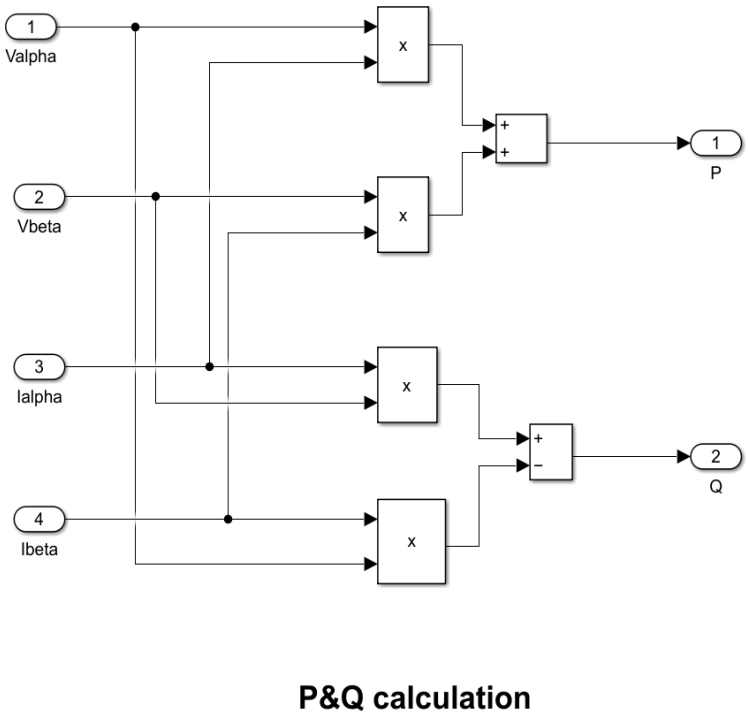


Figure: Active and Reactive Power Calculation Block

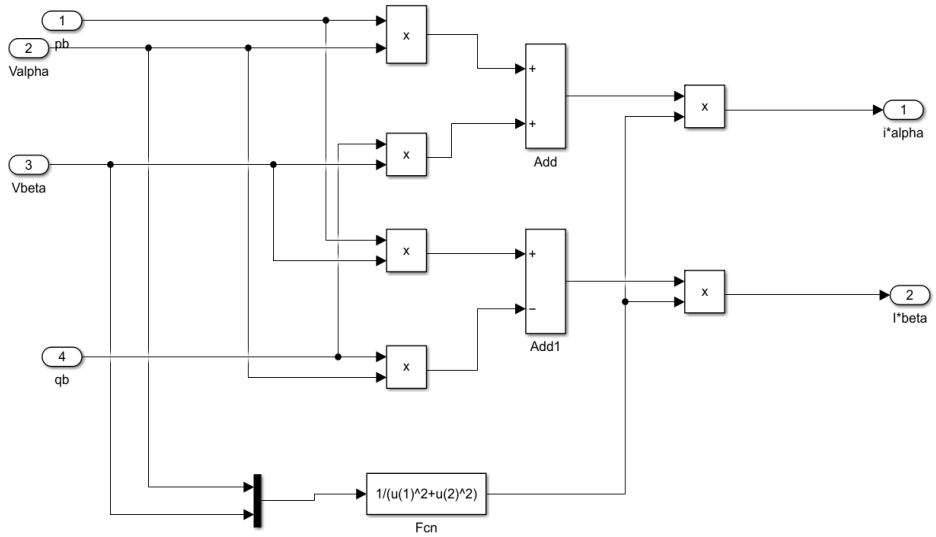


Figure: Reference Current Generation

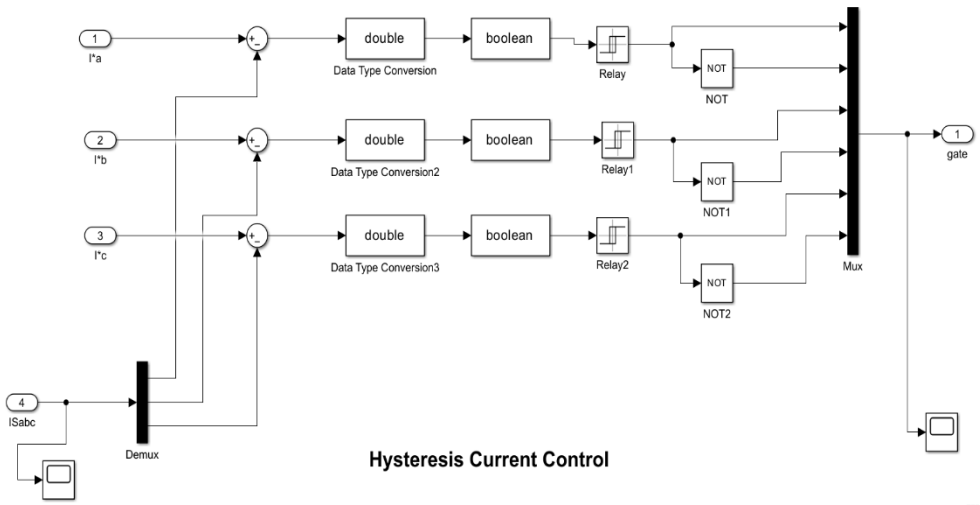


Figure: Hysteresis current control method for switching signals generation

# APPENDIX B: LETTER OF ACCEPTANCE

## IOE GC CONFERENCE ACCEPTANCE

**Notifications** ×

### [IOEGC16] Editor Decision

2025-04-02 08:41 AM

Isha Tiwari:

We are pleased to inform you that your manuscript titled "Harmonic Analysis of Balaju Industrial Feeder" submitted to 16th IOE Graduate Conference is **Accepted** for presentation in the Conference as well as inclusion in the Peer-Reviewed Proceedings. Please note that inclusion in hard copy proceedings is contingent upon your timely response to further edits, if any, during the publication process.

With Warm Regards,
IOEGC-16 Editorial Team

# Harmonic Analysis and Mitigation Strategies for EV Charging Station Integration in Distribution System Network

*Isha Tiwari* [a], *Tek Nath Tiwari* [b], *Laxman Maharjan* [c], *Jeetendra Chaudhary* [d]

**Abstract:**

Electric Vehicles (EVs) are making its way on the mainstream in the automobile industry due to their low CO2 emissions, simple maintenance and low operating costs. As the number of electric vehicles increases, the charging demand affects the distribution network features. The augmentation of electric vehicle infrastructure has brought different challenges in terms of power quality such as harmonic distortion on the distribution network. The employment of modern power electronics equipment in chargers causes variation of loads which is the cause of distortion of normal sinusoidal pattern of the current and voltage waveforms thus leading to hinderance in the system known as harmonics. This research concentrates on analysis of total harmonic distortion (THD) introduced by EVs charging station on real distribution feeder. In this paper, Sanepa distribution feeder is modelled and the shunt active power filter with instantaneous reactive power theory is brought to use allowing to compensate the harmonic currents at the point of common coupling (PCC). The proposed approach is implemented and the outcome shows that the THD is significantly reduced to 1.34% from 31.22%. The modelling and simulation is carried out in MATLAB/Simulink platform.

**Keywords:**

Electric Vehicle, Total Harmonic Distortion(THD), Shunt Active Power Filter, Point of Common Coupling(PCC), Voltage Source Inverter(VSI)

[a] *Department of Electrical Engineering, Pulchowk Campus, IOE, Tribhuvan University, Nepal*

[a] ishatiwari9898@gmail.com

# Harmonic Analysis and Mitigation Strategies for EV Charging Station Integration in Distribution System Network

Isha Tiwari [a], Tek Nath Tiwari [b], Laxman Maharjan [c], Jeetendra Chaudhary [d]

[a] *Department of Electrical Engineering, Pulchowk Campus, IOE, Tribhuvan University, Nepal*
[a] ishatiwari9898@gmail.com

**Abstract**
Electric Vehicles (EVs) are making its way on the mainstream in the automobile industry due to their low CO2 emissions, simple maintenance and low operating costs. As the number of electric vehicles increases, the charging demand affects the distribution network features. The augmentation of electric vehicle infrastructure has brought different challenges in terms of power quality such as harmonic distortion on the distribution network. The employment of modern power electronics equipment in chargers causes variation of loads which is the cause of distortion of normal sinusoidal pattern of the current and voltage waveforms thus leading to hinderance in the system known as harmonics. This research concentrates on analysis of total harmonic distortion (THD) introduced by EVs charging station on real distribution feeder. In this paper, Sanepa distribution feeder is modelled and the shunt active power filter with instantaneous reactive power theory is brought to use allowing to compensate the harmonic currents at the point of common coupling (PCC). The proposed approach is implemented and the outcome shows that the THD is significantly reduced to 1.34% from 31.22%. The modelling and simulation is carried out in MATLAB/Simulink platform.

**Keywords**
Electric Vehicle, Total Harmonic Distortion(THD) , Shunt Active Power Filter, Point of Common Coupling(PCC), Voltage Source Inverter(VSI)

## 1. Introduction

The rising concept of clean and green energy has reduced the use of vehicles powered by fuels. The use of electric vehicles is increasing rapidly compared to internal combustion engine (ICE) vehicles. From the well-to-wheel perspective, the use of EVs reduce Nitrogen oxides by 20 times and particulate matter (PM) by 4 times[1]. Nepal has been making significant strides in promoting electric vehicles (EVs) as part of its commitment to sustainable energy and reducing carbon emissions. In Nepal, the Nepal Electricity Authority (NEA), a government electrical utility company has been at the forefront of this initiative, supporting the development of EV charging infrastructure across the country. There are currently 62 operational EV charging stations under the NEA. NEA has approved applications for an additional 750 charging stations across various locations in Nepal, with a total proposed capacity of 105.32 MW. Of this, 60 MW has already been installed. In total, Nepal has an installed charging capacity of 78.8 MW, collectively supplying an average of 322,300 units of electricity per day(Source-NEA).

The growing market presence of EV charging stations in the distribution system has led to substantial power quality issues, firstly due to harmonic distortions. EV chargers mainly DC chargers employ power electronic converters that introduce non-linear currents, resulting in harmonics that distort the voltage and current waveforms. These harmonics can negatively influence grid performance by increasing THD, causing excessive losses and reduce the lifespan of electrical components such as transformers [2]. Harmonics are non-sinusoidal components in electrical waveforms that arise due to nonlinear loads such as power electronics devices, transformer and fluorescent lighting. In transformers, harmonic voltage causes increase in hysteresis and eddy current losses in the laminations, it also increases stress of the insulation. Harmonic current increases copper loss which increase temperature and create hot spots in that transformer. Harmonics degrade the operating characteristics of protective relays also affects the interruption capability of circuit breakers and fuses[3].

### 1.1 Harmonic Distortion Analysis

The battery of EV needs direct current (DC) for charging. The power electronics converters (non-linear load) convert alternating current (AC) to DC. Hence, the charger circuit topology causes non-linearity of consumed current. Current and voltage waveform can be present as a sum of sinusoidal shapes on different harmonic frequencies. The general distortion level is the total harmonic distortion (THD) level.Total harmonic distortions calculations for voltage and current as a percentage of how much a waveform deviates from a pure sinusoidal signal due to harmonics are expressed in (1) and (2).

$$THD_V = \sqrt{\frac{\sum_{h=2}^{\infty} V_h^2}{V_1}} \tag{1}$$

$$THD_I = \sqrt{\frac{\sum_{h=2}^{\infty} I_h^2}{I_1}} \tag{2}$$

where h – harmonic order number, Vh, Ih – root mean square voltage and current RMS values of main frequency (50 Hz). Harmonics analysis is important to know the condition of

distribution system. Fast Fourier Transform (FFT) is the most powerful tool in mathematics which is widely used for frequency-domain analysis of harmonics. For a continuous-time signal f(t), the Fourier Transform Ff(t) is defined in (3):

$$F(\omega) = \int_{-\infty}^{+\infty} f(t) e^{-j\omega t} dt \tag{3}$$

Where, F(w) is the fourier transform of the time-domain function f(t), f(t) is the original function, w represents the angular frequency in radians per second.

### 1.2 Filter

Filters are used in electrical and electronics systems to remove or reduce unwanted signals, such as harmonics in power systems or noise in communications systems. Conventional passive filters are simple, cost-effective and reliable but have fixed tuning and limited adaptability[4]. Due to the advancement in technologies, the filters used nowadays have dynamic control algorithms to compensate for unwanted signals. Active power filter is an electronic converter that produces and injects into the system the necessary harmonic components to cancel the harmonics of load current. Hybrid active-passive filters combine passive filters with active components for better performance. The literature review reveals that power filters are efficient available technologies that are widely used to eliminate harmonic distortion propagation. Conventionally, series and shunt passive power filters are tied to the distribution network for power quality improvement[5]. However, designing a passive power filter that is capable of efficiently eliminating harmonic current distortion in industrial nonlinear loads connected to a rigid power supply is still a challenge.

### 1.3 Shunt Active Power Filter

Shunt active power filter as depicted in Fig.1 acts as a current source, compensating the harmonic currents due to nonlinear loads. It is composed of two circuits: the power circuit and the control circuit. The power circuit is accountable for synthesizing the required compensation current[6]. It comprises a PWM-based voltage source inverter(VSI) paired with DC-link capacitor to stabilize and regulate the DC voltage. Additionally, the control circuit dynamically monitors the fluctuation in the harmonic current, continuously determining the instantaneous reference compensation current. The shape of compensation current is obtained by measuring load current (iL) and subtracting it from a sinusoidal reference. The aim of shunt APF is to obtain a sinusoidal source current (iS) using the relationship (4):

$$i_S = i_L - i_C \tag{4}$$

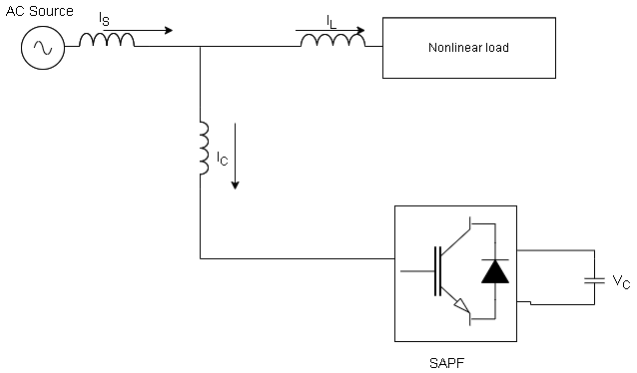


**Figure 1:** Shunt Active Power Filter

### 1.4 Harmonic Detection Strategy

The harmonic extraction assessment plays a crucial role in determining the performance and accuracy of the shunt active power filter. Reference current can be determined through both time domain analysis and frequency domain analysis methods. The PQ theory is grounded on the transformation of the a-b-c stationary reference coordinate to the $0-\alpha-\beta$ rotating coordinate, which is known as a Clarke transformation[7]. The required expressions for source voltages and currents in components $0-\alpha-\beta$ are in (5) and (6):

$$\begin{bmatrix} i_0 \\ i_\alpha \\ i_\beta \end{bmatrix} = \sqrt{\frac{2}{3}} \cdot \begin{bmatrix} 1/\sqrt{2} & 1/\sqrt{2} & 1/\sqrt{2} \\ 1 & -1/2 & -1/2 \\ 0 & \sqrt{3}/2 & \sqrt{3}/2 \end{bmatrix} \cdot \begin{bmatrix} i_a \\ i_b \\ i_c \end{bmatrix} \tag{5}$$

$$\begin{bmatrix} v_0 \\ v_\alpha \\ v_\beta \end{bmatrix} = \sqrt{\frac{2}{3}} \cdot \begin{bmatrix} 1/\sqrt{2} & 1/\sqrt{2} & 1/\sqrt{2} \\ 1 & -1/2 & -1/2 \\ 0 & \sqrt{3}/2 & \sqrt{3}/2 \end{bmatrix} \cdot \begin{bmatrix} v_a \\ v_b \\ v_c \end{bmatrix} \tag{6}$$

With the presence of nonlinear loads, the instantaneous active and reactive power components are decomposed of their AC and DC parts. The Fig.2 below shows the complete control algorithm describing the harmonic current compensation:

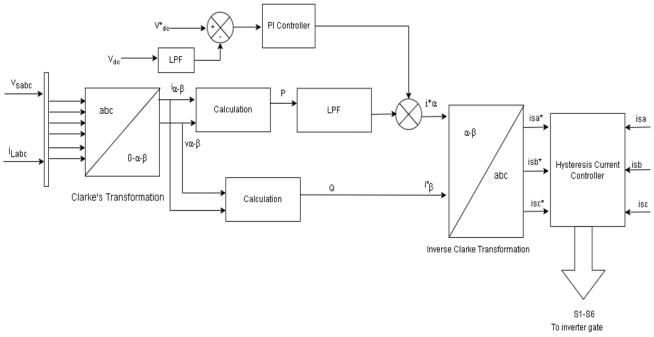


**Figure 2:** Control algorithm using instantaneous reactive power theory

Various control methods have been applied to generate the control pulses for defining the filter switching states. Reference [8] applies hysteresis band current method to

produce switching signals of the voltage source inverter. In this approach, the current is maintained within a predefined band around the reference current. Actual current is compared to the reference current and the inverter switches are turned on and off continuously. With the increasing EV adoption, the authors in [4] highlight the development of an optimal PI controller using a Criminal Search Optimization Algorithm (CSOA). This approach significantly enhances DC-link voltage regulation and improves power quality in EV charging stations. The author of paper[9] advances the field by proposing an analytical model to estimate SAPF capacity based on harmonic parameter estimation and analytical modeling, validated through simulation and real-world testing at an EV charging station. Researchers have developed both DC and AC charging pile circuit models[10] which help in analyzing the electrical characteristics of charging infrastructure. Additionally, this paper have focused on the noise created by charging piles, investigating both conducted and radiated electromagnetic interference (EMI) to assess their impact on the power system and surrounding equipment. [11]analyzes the harmonic currents, apparent, active, reactive and distortion power associated with a cluster of electric vehicle taper-current type battery chargers, connected to a common bus. Harmonic distortion varies significantly across different EV models, often exceeding IEC limits under some conditions. The superposition of harmonics can arise from a wide range of distorting loads, including home and office appliances, as well as equipment, characterized by a substantial penetration into the AC grid[12].

## 2. Methodology

Fig.3 outlines a structured process for analyzing and mitigating harmonic distortion in an electrical feeder with an EV charging station using MATLAB/Simulink. The process begins with a literature review to understand power quality, harmonic distortion, and mitigation techniques. Next essential data, including (i.e. transformer specifications, line length, load details and charger characteristics) were collected to build an accurate system model. A simulation model is then developed in MATLAB/Simulink, incorporating the grid, feeder, and charging station. The simulation is executed to analyze the harmonic distortion. The THD is then compared with IEEE standards to determine compliance. If THD exceeds acceptable limits, a SAPF is designed and integrated into the model to mitigate harmonics. After implementing the filter, the simulation is re-run, and the model results are analyzed to verify the reduction in THD. Finally, the entire process, including data collection, simulation setup, THD analysis and SAPF performance evaluation is thoroughly documented for validation.

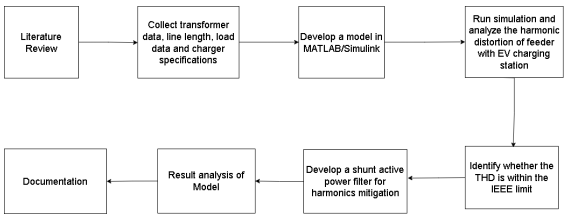


**Figure 3:** Flowchart for Research Work

### 2.1 Data Collection

The EV charging stations are to be provided with 3-phase, 400V, 50Hz AC supply through the distribution transformers connected at 11kV feeder line as per the NEA specifications. This work conducts the study of total harmonic distortion on sanepa distribution feeder of Kathmandu valley due to electric vehicle charging station. The feeder is supplied by Thapathali Switching Station. This feeder consists of 20 transformers and the feeder length is 9.6km. This 11kV system consists commercial as well as residential loads. The Fig.4 shows GIS map view:

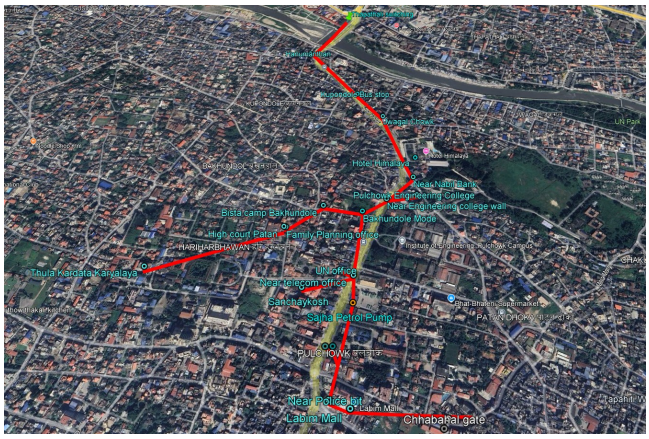


**Figure 4:** GIS map view of sanepa feeder

### 2.2 System Modelling

The feeder is modelled in MATLAB/Simulink environment. Initially, the model was developed to analyze the system behavior before sajha charging station was integrated and the THD in the grid was evaluated. Subsequently, a charging station load was incorporated at the feeder and THD analysis was performed. To mitigate the harmonic distortion introduced due to charging station, a shunt active power filter is designed and connected in parallel. The input voltage for the charger is 380V AC with a tolerance of ±15%. The output voltage varies between 200 and 750V DC while the maximum output current is 150A DC. The charger has an output power of 90KW. The rated frequency ranges from 45Hz to 65Hz data which is shown in Table.1.

**Table 1:** Charger Specifications

| Parameters | Values |
|---|---|
| Input Voltage | 380V±15% AC |
| Input Current | 131A AC max |
| Rated Frequency | 45-65 Hz |
| Output Voltage | 200 ~ 750 $V$ DC |
| Output Current | 150A DC max |
| Output Power | 90KW |
| Ambient Temperaure | $-30^{\circ}$C ~ $+55^{\circ}$C |

Table. 2 specify the electrical characteristics of the power system. The main source voltage is 11kV. A transformer with a rating of 11kV/0.4kV is used to step down the voltage from 11kV to 400V for load-side applications. The load-side AC voltage is maintained at 400V which is suitable for EV charging station. The system frequency is 50Hz. An AC inductor of

1.5mH is included, which helps in filtering harmonics current flow. The power electronic converters or filters in the system operate at the switching frequency of 10kHz.

**Table 2:** Related parameters of feeder and filter

| Feeder Parameters | Values |
|---|---|
| Main source voltage | 11kV |
| System frequency | 50Hz |
| Transformer | 11/0.4 kV |
| Load side voltage | 400V |
| AC inductor | 1.5mH |
| Switching Frequency | 10KHz |

## 3. Results and Discussion

At first, the system was tested for the condition before the charging station was integrated. Sanepa feeder is an urban area in which a lot of other commercial buildings and non-linear loads are also present. The Fig.5depicts the three-phase distorted source current for the scenario before charging station was established. Fig.6 characterizes the total THD for the system before sajha charging station was built which was 9.43%.

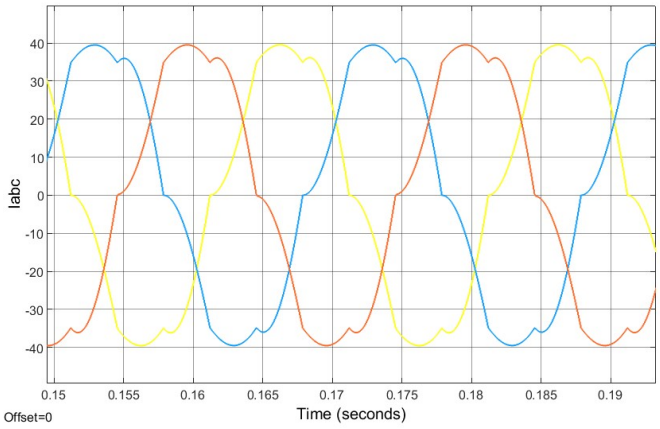


**Figure 5:** Distorted source current before charging station

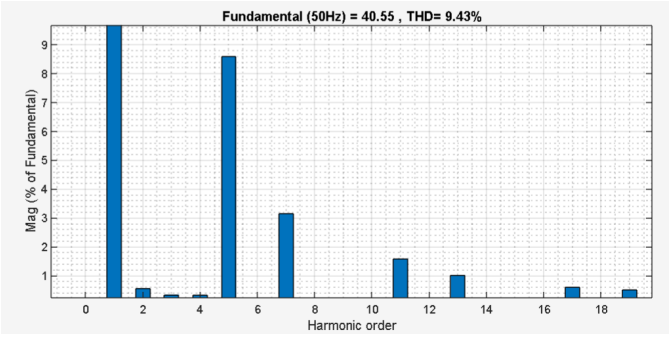


**Figure 6:** THD of system before connecting charging station

For the charging station a 11/0.4 kV transformer is used to step-down the voltage. The source voltage waveform is shown in Fig.7.

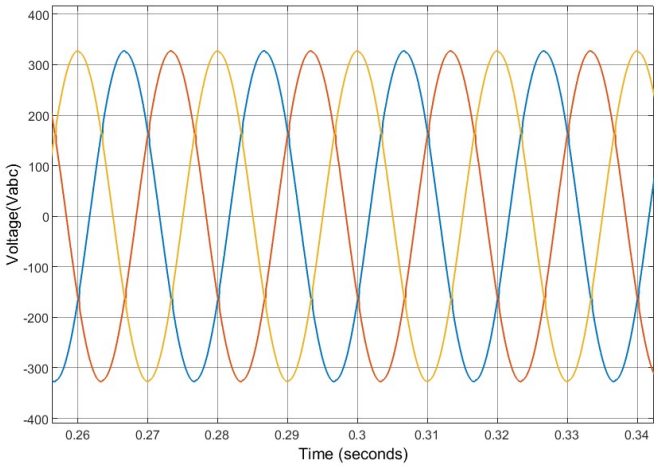


**Figure 7:** Waveform of source voltage

After connecting the charging station to the system, the presence of power electronic converters further distorted the current compared to original current. Fig.8 and Fig.9 shows the waveforms for distortion of three-phase load and source currents.

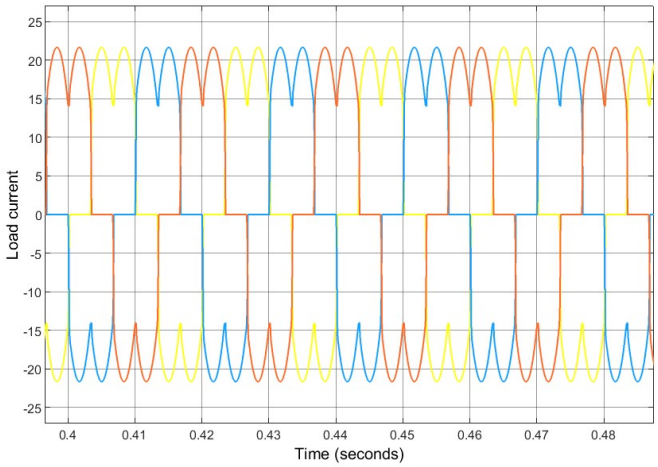


**Figure 8:** Waveform of load current after connecting charging station

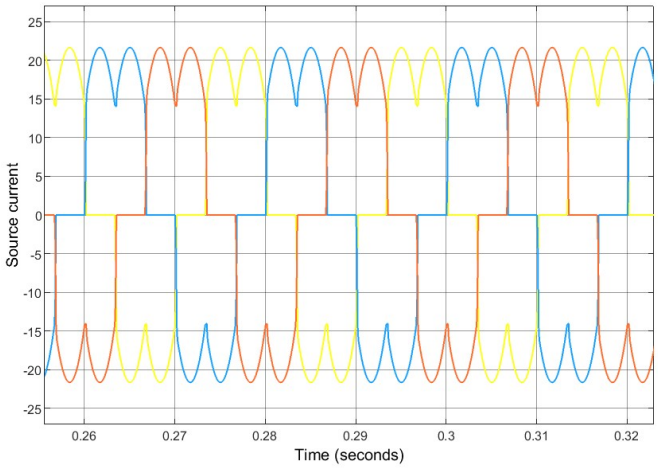


**Figure 9:** Waveform of source current after connecting charging station

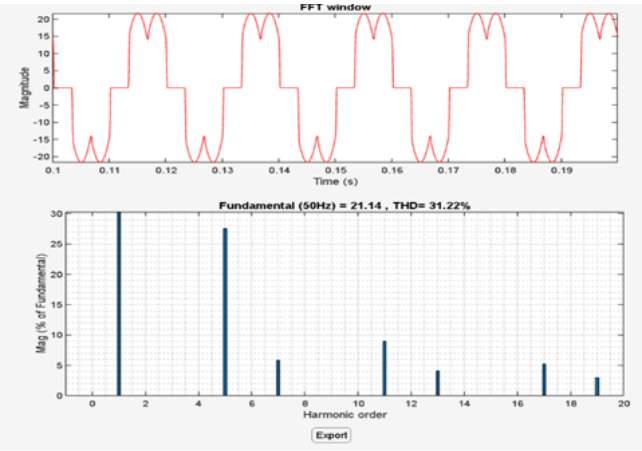


**Figure 10:** FFT analysis of source current before compensation

The source current is distorted due to the non-linearity behavior of the charging stations which contains ac-dc rectifier for converting the utility source voltage to dc form and dc-dc converter to buck/boost the voltage level according to the battery. Fig.10 depicts the Fast Fourier Transform (FFT) analysis for the total harmonic distortion (THD) of the source current as 31.22%, which exceeds the IEEE harmonic standard limit. The dominant harmonics are 5th, 7th, 11th, 13th and 17th respectively.
Fig.11 describes the compensated source current of phase 'a' after connecting the shunt active power filter. The filter provided the compensating harmonics current equal to the distorted current making it more sinusoidal.

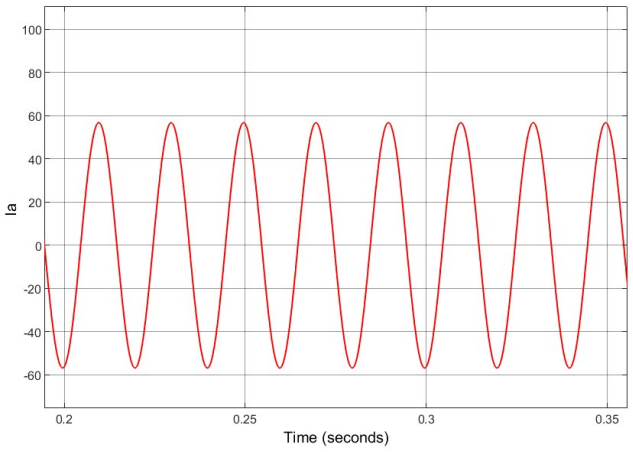


**Figure 11:** Waveform of source current after connecting filter

The THD of the system is beyond IEEE limit and to prevent it a shunt active power filter is connected to the point of common coupling (PCC). Instantaneous reactive power theory control algorithm is used to provide the reference current equal to the harmonic current to make the source current more sinusoidal. Fig.12 portrays Simulink model of the reference compensation current generation (I*a, I*b and I*c) in a-b-c frame respectively.

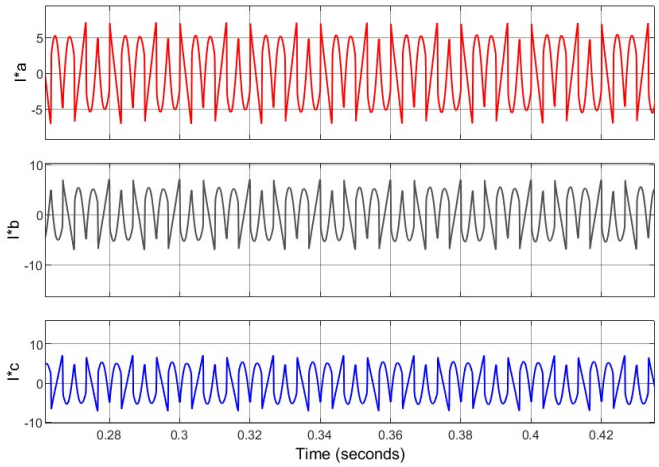


**Figure 12:** Transformed reference current in abc frame

Fig.13shows the THD of the system after connecting the shunt active power filter at the point of common coupling. It reduces the total harmonic distortion to 1.34% from 31.22% which is within the grid code[13] IEEE limit.

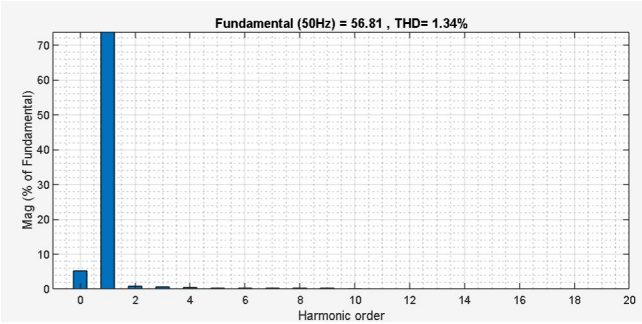


**Figure 13:** Source current FFT analysis after compensation

After the reduction of the total harmonic distortion of the system, the source current becomes sinusoidal which is illustrated in Fig.11.

## 4. Conclusion

There is an increasing trend of electric vehicle globally as well as in Nepali automotive industry. In this study, a modelling of a sanepa distribution feeder is done where there are charging stations located. Involvement of power electronics converters in charging topology acts as a non-linear load which actively brings distortion in the current and voltage waveforms. The simulation results demonstrate that integrating charging stations in large scale significantly injects harmonics current distorting the current waveform. On doing the fast fourier transform analysis before compensation as shown in Fig.11 the total harmonic distortion raised to 31.22% in form of different scale of harmonics which is very high than IEEE limit. Shunt active power filter proposed in this paper is a viable solution to compensate such distortion present in the system. After the use of filter the total harmonic distortion was reduced to 1.34%. This suggests that the use of shunt active power filter proves to provide superior performance, compensating for harmonics in real-time and ensuring compliance with IEEE 519 standards.

Future works will focus on techno-economic assessment of SAPFs by making their control algorithms more advanced. And as smart grids are becoming more prevalent, the application of SAPFs in real-time harmonic mitigation and how they can communicate with other smart grid elements to ensure power quality shall be further explored.

## Acknowledgments

This study was supported by Department of Electrical Engineering, Pulchowk Campus, Nepal Electricity Authority and Sajha Yatayat.

## References

[1] Z Li. A review of the current status of global electric vehicle charging infrastructure development. *International Journal of Global Economics and Management*, 3(3):123–134, 2024.

[2] PT Staats, WM Grady, A Arapostathis, and RS Thallam. A statistical analysis of the effect of electric vehicle battery charging on distribution system harmonic voltages. *IEEE Transactions on Power Delivery*, 13(2):640–646, 1998.

[3] Ewald F Fuchs and Mohammad AS Masoum. *Power quality in power systems and electrical machines*. Academic press, 2011.

[4] Abhishek Srivastava and S Saravanan. Harmonic mitigation using optimal active power filter for the improvement of power quality for a electric vehicle changing station. *e-Prime-Advances in Electrical Engineering, Electronics and Energy*, 8:100527, 2024.

[5] Zainal Salam, Perng Cheng Tan, and Awang Jusoh. Harmonics mitigation using active power filter: A technological review. *Elektrika Journal of Electrical Engineering*, 8(2):17–26, 2006.

[6] Amir A Imam, R Sreerama Kumar, and Yusuf A Al-Turki. Modeling and simulation of a pi controlled shunt active power filter for power quality enhancement based on pq theory. *Electronics*, 9(4):637, 2020.

[7] Fang Zheng Peng and Jih-Sheng Lai. Generalized instantaneous reactive power theory for three-phase power systems. *IEEE transactions on instrumentation and measurement*, 45(1):293–297, 1996.

[8] Zoubir Chelli, Riad Toufouti, Amar Omeiri, and Salah Saad. Hysteresis control for shunt active power filter under unbalanced three-phase load conditions. *Journal of Electrical and computer Engineering*, 2015(1):391040, 2015.

[9] Niancheng Zhou, Jiajia Wang, Qianggang Wang, Nengqiao Wei, and Xiaoxuan Lou. Capacity calculation of shunt active power filters for electric vehicle charging stations based on harmonic parameter estimation and analytical modeling. *Energies*, 7(8):5425–5443, 2014.

[10] L Shang, L Wang, and L Niu. 2020 ieee/ias industrial and commercial power system asia (i&cps asia). 2020.

[11] JA Orr, AE Emanuel, and KW Oberg. Current harmonics generated by a cluster of electric vehicle battery chargers. *IEEE Transactions on Power Apparatus and Systems*, (3):691–700, 1982.

[12] Andrea Mariscotti. Harmonic and supraharmonic emissions of plug-in electric vehicle chargers. *Smart Cities*, 5(2):496–521, 2022.

[13] Christopher K Duffey and Ray P Stratford. Update of harmonic standard ieee-519: Ieee recommended practices and requirements for harmonic control in electric power systems. *IEEE Transactions on Industry Applications*, 25(6):1025–1034, 1989.

## APPENDIX C: PLAGIARISM TEST

# Isha Tiwari

## ISHA_FINAL.pdf

Tribhuvan University

### Document Details

Submission ID
trn:oid:::3117:451404394

Submission Date
Apr 22, 2025, 6:50 PM GMT+5:45

Download Date
Apr 22, 2025, 6:53 PM GMT+5:45

File Name
ISHA_FINAL.pdf

File Size
1.2 MB

42 Pages

10,195 Words

57,766 Characters

# 13% Overall Similarity

The combined total of all matches, including overlapping sources, for each database.

## Match Groups

**134** Not Cited or Quoted 13%
Matches with neither in-text citation nor quotation marks

**0** Missing Quotations 0%
Matches that are still very similar to source material

**0** Missing Citation 0%
Matches that have quotation marks, but no in-text citation

**0** Cited and Quoted 0%
Matches with in-text citation present, but no quotation marks

## Top Sources

7% Internet sources
10% Publications
0% Submitted works (Student Papers)

## Integrity Flags

**1 Integrity Flag for Review**

**Replaced Characters**
18 suspect characters on 6 pages
Letters are swapped with similar characters from another alphabet.

Our system's algorithms look deeply at a document for any inconsistencies that would set it apart from a normal submission. If we notice something strange, we flag it for you to review.

A Flag is not necessarily an indicator of a problem. However, we'd recommend you focus your attention there for further review.

## Match Groups

- **134** Not Cited or Quoted 13%
  Matches with neither in-text citation nor quotation marks
- **0** Missing Quotations 0%
  Matches that are still very similar to source material
- **0** Missing Citation 0%
  Matches that have quotation marks, but no in-text citation
- **0** Cited and Quoted 0%
  Matches with in-text citation present, but no quotation marks

## Top Sources

- 7% Internet sources
- 10% Publications
- 0% Submitted works (Student Papers)

## Top Sources

The sources with the highest number of matches within the submission. Overlapping sources will not be displayed.

| | | |
|---|---|---|
| 1 | Internet | |
| www.mdpi.com | | <1% |
| 2 | Internet | |
| vsip.info | | <1% |
| 3 | Publication | |
| Amir A. Imam, R. Sreerama Kumar, Yusuf A. Al-Turki. "Modeling and Simulation of... | | <1% |
| 4 | Internet | |
| www.jetir.org | | <1% |
| 5 | Internet | |
| www.ijert.org | | <1% |
| 6 | Publication | |
| Power Systems, 2007. | | <1% |
| 7 | Publication | |
| Surajit Chattopadhyay, Madhuchhanda Mitra, Samarjit Sengupta. "Electric Power ... | | <1% |
| 8 | Publication | |
| Gaurava Deep Srivastava, Rajendrakumar D. Kulkarni. "Design, simulation and an... | | <1% |
| 9 | Publication | |
| SHAILENDRA KUMAR JAIN, PRAMOD AGARWAL. "Design Simulation and Experime... | | <1% |
| 10 | Publication | |
| Arindam Ghosh, Gerard Ledwich. "Power Quality Enhancement Using Custom Po... | | <1% |

| | | |
|---|---|---|
| 11 | Publication | Khan, Md. Abdesh Shafiel Kafiey. "A wavelet based speed controller for interior p... <1% |
| 12 | Publication | Mahesh Kumar Mishra. "Power Quality in Power Distribution Systems - Concepts ... <1% |
| 13 | Internet | 1library.net <1% |
| 14 | Publication | Alsharif, Bandar S.. "The Influence of Loading and Voltage Supply Conditions LV F... <1% |
| 15 | Publication | J. C. Das. "Power System Harmonics and Passive Filter Designs", Wiley, 2015 <1% |
| 16 | Internet | elibrary.tucl.edu.np <1% |
| 17 | Internet | coursetakers.com <1% |
| 18 | Internet | mdpi-res.com <1% |
| 19 | Publication | M.A. Rahman. "Performance of current controllers for VSI-fed IPMSM drive", Conf... <1% |
| 20 | Internet | audiolover.com <1% |
| 21 | Internet | info.daviscollege.edu <1% |
| 22 | Internet | utpedia.utp.edu.my <1% |
| 23 | Publication | Rameshchandra, Gupta Vinodkumar. "Novel technique for improving power quali... <1% |
| 24 | Publication | Ewald F. Fuchs, Mohammad A.S. Masoum. "The roles of filters in power systems a... <1% |

25 Publication

R. Sastry Vedam, Mulukutla S. Sarma. "Power Quality - VAR Compensation in Pow... <1%

26 Internet

dpi-journals.com <1%

27 Internet

hdl.handle.net <1%

28 Publication

J. Mahdavi, M. Ehsani. "Power System Harmonic Control", Wiley, 1999 <1%

29 Publication

MANNARI, Keisuke, Yoshiharu ASANO, and Hideki TAKAMURA. "DEVELOPMENT A... <1%

30 Publication

N.F. Guerrero-Rodríguez, Vrindarani Nuñez-Ramírez, Rafael Omar Batista-Jorge, R... <1%

31 Publication

Rahul Raman, Pradip Kumar Sadhu, Ritesh Kumar, Shriram Srinivasarangan Rang... <1%

32 Publication

Vijayakumar Gali, Nitin Gupta, Prashant Kumar Jamwal, Manoj Kumawat, B. Chitti... <1%

33 Internet

link.springer.com <1%

34 Internet

lte.techfak.uni-erlangen.de <1%

35 Internet

www.bou.or.ug <1%

36 Internet

www.idc-online.com <1%

37 Internet

ijpeds.iaescore.com <1%

38 Internet

koreascience.kr <1%

39 Internet
research.riphah.edu.pk <1%

40 Internet
slideplayer.com <1%

41 Internet
worldwidescience.org <1%

42 Internet
www.coursehero.com <1%

43 Internet
www.journal.esrgroups.org <1%

44 Publication
Arrillaga. "Effects of Harmonic Distortion", Power System Harmonics, 09/26/2003 <1%

45 Publication
Diptimayee Swain, Sushree, Pravat Kumar Ray, and K. B. Mohanty. "Voltage comp... <1%

46 Internet
bura.brunel.ac.uk <1%

47 Internet
eprints.nottingham.ac.uk <1%

48 Internet
ijrti.org <1%

49 Publication
Chandwani, Hina B.. "Analysis, design, simulation and implementation of DSP bas... <1%

50 Publication
E FUCHS. "Unified Power Quality Conditioner (UPQC)", Power Quality in Power Sys... <1%

51 Publication
S.Z. Djokic, J.V. Milanovic, D.S. Kirschen. "Sensitivity of AC Coil Contactors to Volta... <1%

52 Publication
Victor Giurgiutiu, Sergey Edward Lyshevski. "Micromechatronics - Modeling, Anal... <1%

53 Publication
G. Chen, K.M. Smedley. "Steady-State and Dynamic Study of One-Cycle-Controlled ... <1%

54 Publication
Gaber Ahmed, Fareed Mohamed, Mohamed Nosier. "Power quality improvement ... <1%

55 Publication
Karuppanan, P, and Kamala Kanta Mahapatra. "PLL with fuzzy logic controller ba... <1%

56 Publication
Sanjeev Rajput, Ravi Kant Pathak. "Seismic Exploration to Reservoir Excellence", S... <1%

57 Publication
Shunliang Wang, Haijun Liu, Junpeng Ma, Lin Feng, Tianqi Liu, Zihao Wu, Ruogu ... <1%

58 Publication
Yahya Naderi, Seyed Hossein Hosseini, Saeid Ghassem Zadeh, Behnam Mohamm... <1%

59 Internet
docplayer.fi <1%

60 Internet
fastercapital.com <1%

61 Internet
ia601709.us.archive.org <1%

62 Internet
ndl.ethernet.edu.et <1%

63 Internet
repository.effatuniversity.edu.sa <1%

64 Publication
"Advanced Control Engineering Methods in Electrical Engineering Systems", Sprin... <1%

65 Publication
Jirayus Arbking, Wira Srimala, Apisit Saengsai, Athita Onuean. "Recommendation ... <1%

66 Publication
M.A. Rahman, G.H. George, T.S. Radwan, M.N. Uddin. "Performance of current co... <1%